Aus dem Fachgebiet für Neuropathologie

(Leiter: Univ.-Prof. Dr. J. Schlegel)

des

Instituts für Allgemeine Pathologie und Pathologische Anatomie

der Technischen Universität München

(Direktor: Univ.-Prof. Dr. H. Höfler)

Targeting heterodimeric EGFR/ErbB2-receptor complexes with novel bispecific small-molecule tyrosine kinase inhibitors in combination with an experimental radiotherapy in human malignant glioma cells

Sabina Berezowska

Meiner Familie und meinen Freunden.

Table of contents

1.   Abbreviations

ABL	Abelson kinase gene
A.d.	Aqua dest.
Akt	serine/threonine-specific protein kinase, encoded by the oncogene Akt (also called Akt1), originally identified as the oncogene in the transforming retrovirus AKT8
APS	Ammonium persulfate
ATP	Adenosine triphosphate
BCR-ABL	fusion gene of breakpoint cluster region (BCR) and ABL
BSA	bovine serum albumin
CML	Chronic myeloid leukaemia
DMEM	Dulbecco's modified Eagle medium
DMSO	dimethyl sulfoxide
DTT	Dithiothreitol
ECL	Enzymatic Chemiluminescence
EDTA	ethylenediaminetetraacetic acid
e.g.	*exempli gratia*
EGF	Epidermal growth factor
EGFR	Epidermal growth factor receptor
EGTA	Ethylene glycol-bis(beta-aminoethyl ether)-N,N,N',N'-tetraacetic acid
ErbB1-4	tyrosine kinase receptor family, encoded by the oncogenes c-erbB 1 – 4, originaly named due to their homology to the **er**ythro**b**lastoma viral gene product *v-erbB*
FACS	Fluorescence activated cell sorting
FBS	Fetal bovine serum
Fig.	Figure
GBM	Glioblastoma
Gy	Gray
HCl	Hydrochloric acid
i.e.	*id est*
IgG	Immunoglobulin G
IP	Immunoprecipitation

LOH	Loss of heterozygosity
M	molar
MAPK	Mitogen-activated protein kinases
MDM2	murine double minute 2
MEK	Mitogen-activated protein kinases kinase
MGMT	O^6-methylguanine-DNA methyltransferase
NaCl	Sodium chloride
NaF	Sodium fluoride
NRGs	Neuregulins
PBS	phosphate buffered saline
PI3K	Phosphatidylinositol 3-kinase
PIP2	Phosphatidylinositol (4,5) bisphosphate
PIP3	Phosphatidylinositol (3,4,5) trisphosphate
PMSF	Phenyl-methyl-sulfonyl-fluoride, a serine protease inhibitor
PTEN	Phosphatase and tensin homologue deleted on chromosome ten
PVDF	Polyvinylidene difluoride
RTK	Receptor tyrosine kinase
SDS	Sodium dodecyl sulfate
SDS-PAGE	SDS polyacrylamide gel electrophoresis
TBS	Tris Buffered Saline
TEMED	Tetramethylethylenediamine
TGFα	Transforming growth factor alpha
TKI	small-molecule tyrosine kinase inhibitor
Tris	tris (hydroxymethyl) aminomethane
Tween 20	Polyoxyethylene sorbitan mono-laurate
TTBS	Tween-Tris Buffered Saline
VEGF	vascular endothelial growth factor
WHO	World Health Organisation
wt	wildtype

2. Introduction

2.1. WHO classification of astrocytic tumors

Glioblastoma (Astrocytoma WHO grade IV) is the most frequent (60 − 75 %) and most malignant histological form of astrocytic glial tumors, which as a group account for about 45 % of primary intracerebral neoplasms (Ohgaki and Kleihues, 2005). Aside from the rare occurrence of familial brain tumors (e.g. neurofibromatosis 1 or 2), which constitute less than 1 % of all the patients with gliomas, the etiology of the disease remains unknown. GBM is generally accepted to develop through dedifferentiation from mature astrocytes (Louis et al., 2007). Although some argue for its origin from neural stem cells, proof for this theory still remains to be found (Jordan et al., 2006; Mayer-Proschel et al., 1997).

According to the histopathological classification by the WHO, astroglial tumors are graded from grade I to IV (Louis et al., 2007). Grade I astrocytomas are slowly growing and well-circumscribed lesions regarded as benign. Grade II-IV astrocytic tumors are diffusely infiltrative malignant lesions, showing cytological atypia only (grade II), along with anaplasia and mitotic activity (grade III) or with additional microvascular proliferation and/or necrosis (grade IV) (Louis et al., 2007) (Table 2.1.).

Contrary to benign grade I astrocytomas, which only very rarely undergo malignant transformation (Tomlinson et al., 1994), grade II and III astrocytomas tend to progress malignantly, a significant proportion ultimately attaining grade IV status. Typical patient survival times range from more than 5 years for grade II tumors and 2-3 years for grade III neoplasms. The majority of glioblastoma patients (grade IV) succumb to the disease within a year (Louis et al., 2007).

Astrocytic tumors	WHO Grading			
	I	II	III	IV
Subependymal giant cell astrocytoma	●			
Pilocytic astrocytoma	●			
Pilomyxoid astrocytoma		●		
Diffuse astrocytoma		●		
Pleomorphic xanthoastrocytoma		●		
Anaplastic astrocytoma			●	
Glioblastoma				●
Giant cell glioblastoma				●
Gliosarcoma				●

Table 2.1. WHO Grading of astrocytic tumors. Modified from Louis et al., 2007.

2.2.   Glioblastoma (GBM) – current therapeutic approach

Standard treatment of glioblastoma generally consists of cytoreductive surgery followed by radiotherapy and chemotherapy. When feasible, maximal surgical resection of tumor improves survival (Lacroix et al., 2001), but complete resection is virtually impossible due to the highly infiltrating nature of the neoplasm. And although a putatively clear magnetic resonance image postoperatively may nourish hope, tumor cells invariably persist and trigger recurrence at the initial site or distally, sometimes even in the contralateral hemisphere. This renders additional postoperative treatment exceptionally desirable.

For a long time radiation was the only main adjuvant therapeutic option, resulting in a modest median survival improvement of less than 6 month in all age groups (Grossman and Batara, 2004; Keime-Guibert et al., 2007). Since only recently standard treatment comprises the combination of radio-/chemotherapy, as it was reported that adjunctive chemotherapy with the alkylating agent temozolomide improved median survival time by 2.5 month compared to radiotherapy alone (Stupp et al., 2005). In particular a subgroup of patients with epigenetic silencing of the MGMT (O^6-methylguanine-DNA methyltransferase) DNA-repair gene by promotor methylation was shown to benefit most from radio-/chemotherapy, reaching a median survival of 21.7 month compared to 15.3 month after adjuvant radiotherapy alone (Hegi et al., 2005). But in spite of all efforts to improve radiation and chemotherapy protocols, up to date the treatment of glioblastoma remains palliative and – most importantly – the prognosis of patients has changed very little. Consequentially, novel therapeutic agents and approaches are especially desirable in the treatment of this devastating disease.

Novel highly promising oncological therapies under development target and inhibit the activities of specific molecules that contribute to the malignancy and radioresistance of malignant neoplasms. This approach already resulted in valuable clinically approved pharmacological agents. Perhaps the first success story was a selective inhibitor of the ABL tyrosine kinase (Imatinib mesylate/Glivec®), which proved effective in putting nearly all patients with BCR-ABL-driven chronic-phase CML into complete remission (Kantarjian et al., 2002). This proof of concept edified the image of "oncogenic addiction", the dependence of tumor cells on specific molecular events (Weinstein, 2002), and brings hope to the treatment of other hematologic and solid tyrosine-kinase driven tumors. In particular, in the present work it was exploited in the treatment of glioblastoma, which is known to be driven by the epidermal growth factor receptor (EGFR) tyrosine kinase pathway (Ohgaki and Kleihues, 2007).

2.3. Sub-classification of Glioblastoma

2.3.1. Clinical subgroups of Glioblastoma

GBM incidence peaks among the 50-60 year old, with a male to female ratio of about 1.28 (Switzerland) (Ohgaki and Kleihues, 2005). It can develop along two distinct clinical pathways. The majority of cases (95 %) present *de novo* as primary glioblastoma, with no pathologic precursor lesion, and have a clinical prodrome of less than 3 month. They typically develop in older patients with a mean age of 62 years. In contrast, secondary glioblastomas develop from lower-grade astrocytomas over a 5- to 10-year period, constitute only about 5 % of all GBM cases and affect significantly younger patients with a mean age of 45 years (Dropcho and Soong, 1996; Ohgaki et al., 2004). Mean survival is inversely correlated with age. After correction for age though, it remains controversial whether the prognosis of patients with secondary glioblastoma is better than or similar to the prognosis of patients with primary glioblastoma (Ohgaki et al., 2004).

The clinical distinction of the presently acknowledged *de novo* and secondary GBM subgroups had been made for the first time way back in 1940 (Peiffer and Kleihues, 1999; Scherer, 1940), but it took about half a century and immunohistochemical backing until glioblastoma was even firmly categorized as an astrocytic neoplasm (Kleihues et al., 1993). Being histopathologicaly indistinguishable, the subdivision in *de novo* and secondary lesions is mainly based upon clinical, epidemiological and genetic differences. In particular different genetic alterations present strong evidence that GBM is not a homogenous group of tumors but rather comprised of two very distinct disease entities.

2.3.2. Genetic subgroups of Glioblastoma

De novo and secondary GBM share a set of characteristics crucial to the malignant phenotype, consisting of proliferation in the absence of external growth stimuli, evasion of apoptosis and no limits to replication, escape from external growth-suppressive forces and immune response, sustained angiogenesis, and an ability to invade normal tissue (Hanahan and Weinberg, 2000).

Despite phenotypic similarities and some genetic overlap, the concept of two different genetic pathways leading to the common phenotypic endpoint GBM has gained general acceptance, rendering *de novo* and secondary glioblastoma two different disease entities (Louis et al., 2007; Ohgaki et al., 2004) (Fig. 2.1.).

The EGFR/PTEN/Akt pathway is involved in the control of cell proliferation, and a key signalling pathway in the development of *de novo* GBM (Ohgaki and Kleihues, 2007). The epidermal growth factor receptor (EGFR) is the only member of the ErbB or EGFR family of proteins known to be amplified in a significant number of GBM (Schlegel et al., 1994). Amplification of the EGFR occurs in ~ 40 % of *de novo* GBM but rarely in secondary GBM (Ohgaki et al., 2004). EGFR overexpression is also more common in *de novo* GBM (> 60%) than in secondary GBM (< 10%), independent of amplification status (Watanabe et al., 1996), and is associated with disease progression. It should be noted that expression of ErbB2 (HER2/neu) – another member of the ErbB family of receptors – was observed in the majority of GBM (> 80 %), with high expression patterns detectable only in *de novo* GBM specimens (Mineo et al., 2007).

Multiple genetic EGFR mutations are apparent, including both overexpression of the receptor as well as rearrangements that result in truncated isoforms (e.g. EGFRvIII), both leading to increased activity. GBMs with increased EGFR activity typically show a simultaneous loss of chromosome 10 but rarely a concurrent p53 mutation.

PTEN (Phosphatase and Tensin homolog) – also known as MMAC (mutated in multiple advanced cancers) or TEP1 (TGFβ-regulated and epithelial-cell enriched phosphatase) – encodes a tyrosine phosphatase located at band 10q23.3. Its tumor-suppressing action derives from turning off the Akt signalling pathway downstream to EGFR. When PTEN phosphatase activity is lost because of genetic mutation, the Akt signalling pathway can become activated constitutively, resulting in aberrant proliferation. PTEN mutations have been found in as many as 25 % of *de novo* glioblastomas, but only 8 % of secondary GBM (Ohgaki et al., 2004).

Loss of heterozygosity (LOH) on chromosome arm 10q is the most frequent gene alteration in GBM, occurring in 60 - 90 % of cases at similar frequencies in *de novo* and secondary GBM (Ohgaki et al., 2004). This mutation appears to be a late event in tumorigenesis and is found rarely in other tumor grades of astrocytoma than GBM. It is associated with poor survival.

TP53 mutations are a genetic hallmark of secondary GBM (65 %), and they are usually already present in precursor lower-grade astrocytic lesions (Louis et al., 2007; Watanabe et al., 1996). In *de novo* GBM, mutations or amplifications are more commonly seen in regulators of p53 levels and activity. MDM2 inhibits p53 function and was overexpressed in over 50 % of *de novo* GBM (Biernat et al., 1997). p14^{ARF} negatively regulates the ability of MDM2 to target p53 for degradation, but there was no significant difference in the overall frequency of p14^{ARF} alterations between *de novo* and secondary GBM (50 % versus 75 %) (Nakamura et al., 2001).

Malignant gliomas usually harbour only a single mutation of the p14^{ARF}/MDM2/TP53 cascade, indicating the presence of a linear pathway (Fulci et al., 2000; Rich and Bigner, 2004).
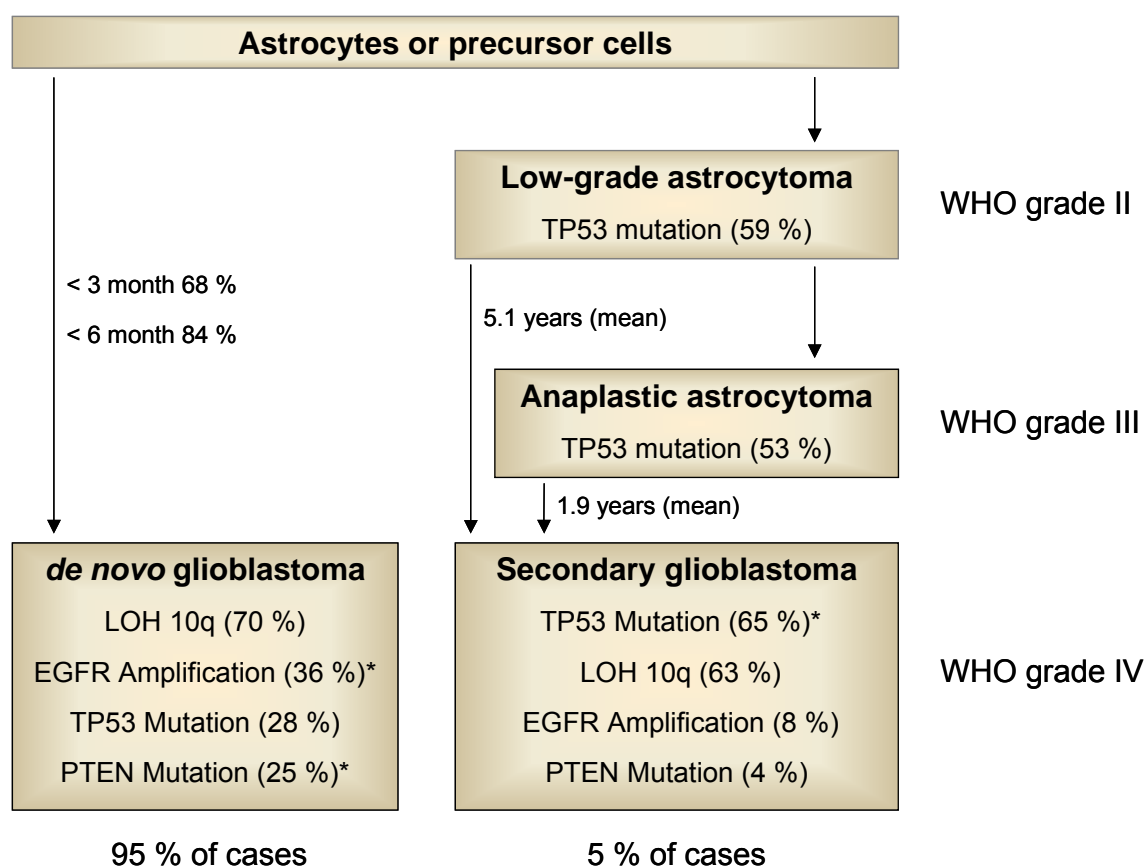
Figure 2.1. Timing and frequency of genetic alterations operative in the evolution of *de novo* and secondary glioblastomas. LOH 10q is frequent in both *de novo* and secondary GBM. TP53 mutations are early and frequent alterations in secondary GBM, whereas alterations of the EGFR pathway including PTEN mutation are significantly more frequent in *de novo* than in secondary GBM. (* = genetic alterations that are significantly different in frequency between *de novo* and secondary GBM). Modified from Ohgaki et al., 2004.

2.4. ErbB-Receptor Family

The ErbB or epidermal growth factor receptor (EGFR) family of proteins belongs to the subclass I of the receptor tyrosine kinase (RTK) superfamily and generates increasing interest as a target for cancer therapeutics as it has been found to play a major role in the pathogenesis of many human malignancies, including breast, lung and head-and-neck cancers and glioblastoma (Kapoor and O'Rourke, 2003).

It was originally named due to its homology to the **er**ythro**b**lastoma viral gene product *v-erbB* and comprises EGFR (ErbB1/HER1), ErbB2 (HER2/neu), ErbB3 (HER3) and ErbB4 (HER4). All four members are close homologs and share common structural elements, like an extracellular ligand-binding domain, a single membrane-spanning region and a cytoplasmic protein tyrosine kinase-containing domain.

Binding of ligands to ErbB receptor monomers induces formation of homo- and heterodimers (Dawson et al., 2005; Ferguson et al., 2003), and as a consequence activates the intrinsic kinase domain with subsequent transphosphorylation on specific tyrosine residues within the cytoplasmic tail of the receptors. These phosphorylated residues serve as docking sites for a variety of signalling molecules which lead to the activation of intracellular pathways (Olayioye et al., 2000; Yarden and Sliwkowski, 2001).

The EGFR, a 170 kDa RTK is activated by six ligands: epidermal growth factor (EGF), transforming growth factor α (TGFα), amphiregulin, heparin-binding EGF-like growth factor, betacellulin and epiregulin. The last three of them show dual specificity, binding both EGFR and ErbB4. ErbB3 and ErbB4 receptors bind neuregulins (NRGs), a family of structurally diverse peptides (Holbro and Hynes, 2004) (Fig. 2.2.). Ligand binding to the monomeric receptor induces rotation of the transcellular domain and extension of the dimerization arm, thereby enabling dimerization, which is subsequently entirely receptor mediated (Citri and Yarden, 2006).

Two members of the ErbB family (ErbB2 and ErbB3) are non-autonomous. The 185 kDa protein ErbB2 lacks the capacity and the necessity to directly interact with a growth-factor ligand (Klapper et al., 1999), as its extracellular dimerization loop is constitutively extended (Garrett et al., 2003). It fails to form homodimers, but serves as a co-receptor forming EGFR/ErbB2 heterodimers when transactivated by EGF-like ligands or ErbB3/ErbB2 or ErbB4/ErbB2 heterodimers induced by neuregulins (Rubin and Yarden, 2001). Interestingly,

ErbB2 constitutes the prefered dimerization partner for all other ErbB receptors, and this preference is further enhanced by overexpression of ErbB2 in human cancer cells (Tzahar and Yarden, 1998). Furthermore and contrary to comparably weak homodimer signalling, ErbB2 containing heterodimers are particularly potent activators of downstream effector pathways through their prolonged signalling due to a relatively slow rate of ligand dissociation, delayed receptor internalization and frequent recycling back to the cell surface instead of receptor degradation (Baulida et al., 1996; Gulliford et al., 1997; Lenferink et al., 1998). Thus, ErbB2 may be regarded as a "non-autonomous amplifier" of the network, rather than an additional growth-factor receptor (Citri and Yarden, 2006).

ErbB3 has a defective kinase activity, rendering its homodimers completely inactive. Induced by neuregulines it gaines function by formation of heterodimers with the other members of the ErbB family (Kim et al., 1998), combination with ErbB2 resulting in the most potent alliance, as described for the other ErbB members.

In conclusion, this elaborated network at the level of signal initiation further highlights the biologic importance of the ErbB receptor family, showing enormous potential for diversification and modulation of biological messages, instead of four linear pathways.
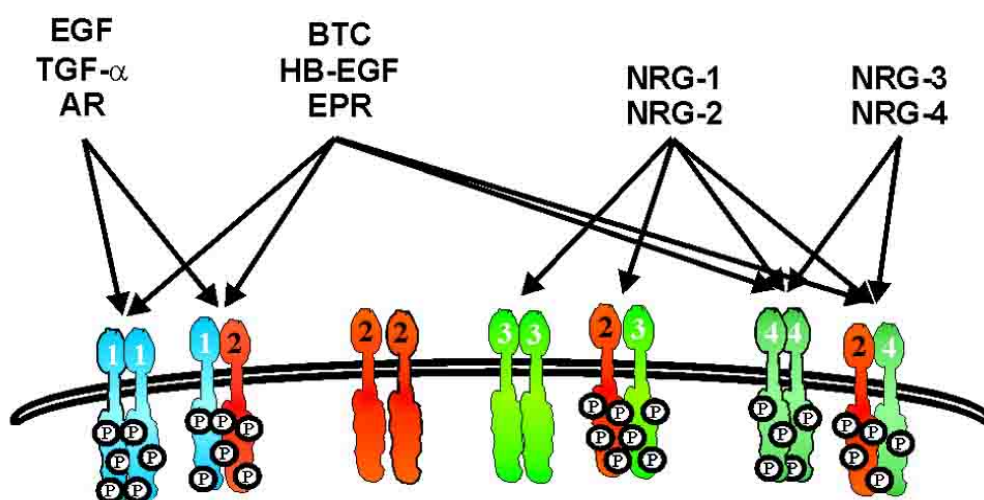
Figure 2.2. The ErbB signalling network (ErbB1-4). Ligands bind to their receptors causing the formation of different dimers. Signalling, induced by transphosphorylation, is indicated by encircled P. ErbB2 has no direct ligand inducing homodimerization and acquires signalling potential through heterodimerization with other ErbB receptors. ErbB3 homodimers are void of signalling potency due to impaired kinase activity.

EGF: Epidermal growth factor; TGF-α: transforming growth factor-α; AR: amphiregulin; BTC: betacellulin; HB-EGF: heparin-binding EGF-like growth factor; EPR: epiregulin; NRG 1-4: neuregulin 1-4. Modified from Holbro and Hynes, 2004.

2.5.   Signalling pathways downstream to ErbB receptors

The ErbB family of receptor tyrosine kinases controls a complex process of lateral signalling through ligand-induced homo- and heterodimerizations (Olayioye et al., 2000). These intra- and inter-receptor interactions define a hierarchical array of possible signalling partners, which greatly complicates efforts to understand their unique functions and pathways. Activated ErbB receptors stimulate a wide range of intracellular pathways, which furthermore show extensive overlap (Yarden and Sliwkowski, 2001). Even though, two main survival-signal transduction-pathways downstream to EGFR and ErbB2-receptors can be identified, their activation causing antiapoptosis, cellular proliferation, migration and invasion.

(a) Grb2 (Growth-factor-receptor-bound-2)/Shc (Src-homology-2-containing) and Sos (Son of sevenless) are responsible for the recruitment of membrane bound Ras which activates the mitogen-activated protein kinase (MAPK) cascade through activation of Raf-1 kinase. Ras-GTP (i.e. activated Ras) is inactivated to Ras-GDP through intrinsic GTPase activity, catalyzed by GTPase-activating proteins. Oncogenic Ras is resistant to Ras GTPase-activating proteins and is therefore locked into its GTP-bound form, resulting in constitutive activation. Though oncogenic Ras is common to other tumors, but not typically observed in GBM, it has been reported that high-grade gliomas commonly have elevated levels of Ras-GTP. Because GBM commonly have overexpression and amplification of receptor tyrosine kinases such as EGFR, this may represent an important mechanism through which Ras signalling is upregulated in GBM. As inhibition of Ras resultes in antiproliferative, antiangiogenic and proapoptotic effects in GBM cell lines and is recognized as a major effector of EGFR signalling, it may represent one major mechanism by which EGFR enhances the malignant potential of GBM cells (Chakravarti et al., 2004a; Kapoor and O'Rourke, 2003).

(b) Activation of the phosphatidylinositol 3-kinase (PI3K)-/Akt pathway has been detected in several types of human malignant neoplasms including gliomas, and found to be associated with poor clinical outcome and resistance to chemotherapy and radiotherapy (Brognard et al., 2001; Ermoian et al., 2002).
Phosphatidylinositol 3-kinase (PI3K) phosphorylates phosphatidylinositol (4,5) bisphosphate (PIP2) to form phosphatidylinositol (3,4,5) trisphosphate (PIP3), which then activates Akt by binding at its pleckstrin homology (PH) domain. Phosphorylated Akt has several effects, both in the cytoplasm and in the nucleus, which include the inhibition of proapoptotic factors such

as BAD (BCL2 antagonist of cell death), procaspase-9 and the Forkhead (FKHR) family of transcription factors (FOXO). Akt-mediated activation of mTOR (mammalian target of rapamycin) is also important in stimulating cell proliferation. PI3K/Akt-mediated activation of VEGF (vascular endothelial growth factor) and HIF1α (hypoxia inducible factor-1α) are important in angiogenesis (Kapoor and O'Rourke, 2003), further enhancing the importance of this pathway for oncogenesis.

It is widely acknowledged that activation of PI3K/Akt is regulated by the lipid phosphatase activity of PTEN, which inhibits Akt activation by converting PIP3 to PIP2, thereby mediating cell cycle arrest and/or apoptosis. Loss of PTEN consequently results in constitutive activation of Akt and thereby triggers aberrant proliferation.

There is extensive crosstalk between MAPK and Akt signalling pathways, which is exemplified by the important propensity of Ras to activate the PI3K/Akt pathway (Kapoor and O'Rourke, 2003).
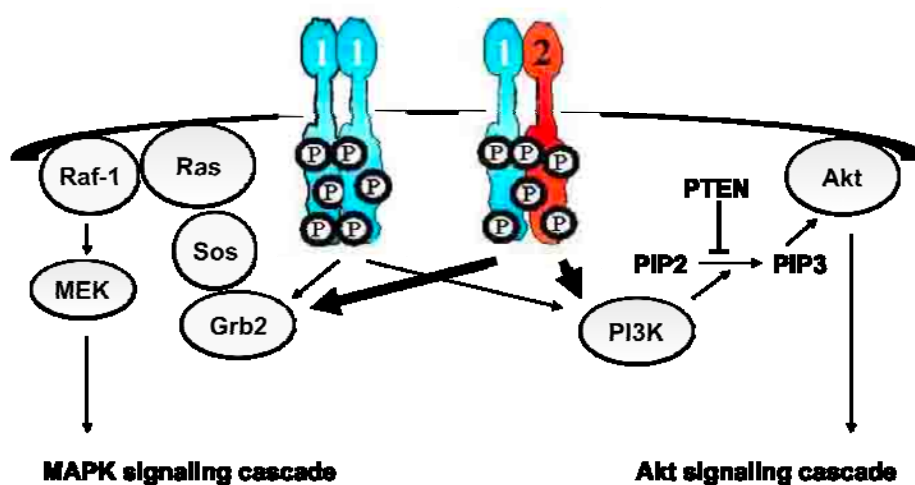
Figure 2.3. The mitogen-activated protein kinase (MAPK)- and the Akt signalling cascades constitute the main signal transduction pathways downstream to ErbB receptors EGFR (ErbB**1**) and ErbB**2**. Bold arrows leading downstream the EGFR/ErbB2-receptor heterodimer represent its superior signalling potency compared to homodimer signalling, represented by thin arrows. Crosstalk between the signalling cascades is not shown for clarity.

Grb2: Growth-factor-receptor-bound-2; Sos: Son of sevenless; Raf-1: rapidly growing fibrosarcoma-1; MEK: MAPK-kinase; MAPK: mitogen-activated protein kinase; PI3K: phosphatidylinositol 3-kinase; PIP2: phosphatidylinositol (4,5) bisphosphate; PIP3: phosphatidylinositol (3,4,5) trisphosphate; PTEN: phosphatase and tensin homologue deleted on chromosome ten. Modified from Holbro and Hynes, 2004 and Mischel and Cloughesy, 2003.

2.6.   Rationale for targeting ErbB receptors in Glioblastoma

The rationale for targeting ErbB protein tyrosine kinases in *de novo* GBM is compelling. As described in chapter 2.3.2. the EGFR pathway is recognized as a key signalling pathway in the development of *de novo* GBM (Ohgaki and Kleihues, 2007), EGFR being amplified or at least overexpressed by the majority of tumors. It is of interest, that in particular *de novo* GBM show a co-expression of the "ErbB network amplifier" ErbB2 (Mineo et al., 2007; Schlegel et al., 1994). Furthermore, the ErbB receptors are known to regulate multiple cellular processes that contribute to tumor development and progression, including cell growth, differentiation, migration, and apoptosis (Olayioye et al., 2000). Thus not surprisingly, EGFR gene amplification and protein overexpression were found to be significantly correlated with disease progression and reduced survival in GBM patients (Chakravarti et al., 2001).

In conclusion, the acknowledged contribution of ErbB or EGFR family signalling pathways in malignant processes, the EGFR deregulation as a hallmark of *de novo* GBM and its adverse prognostic significance make ErbB inhibitors an attractive class of molecularly targeted agents.

2.7.   Rationale for combining ErbB-inhibition with radiotherapy in Glioblastoma

In general, combination of ErbB-inhibition and radiotherapy holds great promise, since ErbB receptors are known to be activated by ionizing radiation to produce downstream cytoprotective effects through Akt and MAPK signalling cascades (Carter et al., 1998; Contessa et al., 2002). Thus, activation of ErbB receptors results in radioresistance and accounts for at least part of "accelerated repopulation", a condition of enhanced cellular proliferation after exposure to ionizing radiation (Nyati et al., 2006; Riesterer et al., 2007; Schmidt-Ullrich et al., 1999).

Radiosensitisation as a therapeutic strategy is of particular interest in the treatment of GBM. While adjuvant radiotherapy remains the single most effective agent, durable tumor control remains elusive. It was shown in preclinical settings that radiation may even enhance invasion of GBM in an Akt and EGFR dependent manner (Zhai et al., 2006). Furthermore, upregulation of EGFR is recognized to contribute to the intrinsic radioresistance of glioblastoma (Chakravarti et al., 2004a). This strengthens the rational for ErbB receptor inhibition as a possible radiosensitizing strategy in GBM.

2.8.   ErbB receptor targeted therapy

Although the disruption of ErbB function can be accomplished by several methods, two approaches have been most extensivly investigated in laboratory and clinical settings, resulting in two major classes of anti-ErbB-therapeutics: (a) ectodomain binding monoclonal antibodies and (b) small-molecule tyrosine kinase inhibitors that compete with ATP in the catalytic tyrosine-kinase domain.

2.8.1.   Monoclonal antibodies (mAbs)

Monoclonal antibodies are directed against the extracellular ligand binding domain of the ErbB receptors. They prevent ligand binding and receptor dimerization and hence activation. Antibodies specific for the extracellular domains of EGFR and ErbB2 have been developed with successful clinical outcomes. The anti-EGFR antibody cetuximab (Erbitux®) was recently FDA-approved for the treatment of colorectal carcinoma and squamous cell carcinoma of the head and neck (Goldberg, 2005; Panikkar et al., 2008), and the anti-ErbB2 antibody trastuzumab (Herceptin®) is now in widespread use in the management of patients with breast cancer (Stebbing et al., 2000).

2.8.2.   Small-molecule tyrosine kinase inhibitors (TKIs)

More recently, small-molecule tyrosine kinase inhibitors (TKIs) have been developed as therapeutic agents. Those compounds are cell-permeable agents that inhibit reversibly or irreversibly the ligand-dependent and -independent protein tyrosine kinase activity of the ErbB-receptors residing within the intracellular domain. This strategy has a solid rational basis since kinase activity is essential for activation of downstream signalling and hence for the oncogenic function of ErbB-receptors (Olayioye et al., 2000; Yarden and Sliwkowski, 2001) (Fig. 2.4.).

Up to date, there are several small-molecule inhibitors in advanced clinical testing or already approved for clinical use (Krause and Van Etten, 2005).

The first EGFR receptor inhibitors, gefitinib (also known as Iressa® or ZD1839) and erlotinib (also known as Tarveca® or OSI-774) have already been approved for refractory locally advanced or metastatic non-small-cell lung cancer (Krause and Van Etten, 2005).

Both compounds have also been tested in high-grade glioma patients (Table 2.2.). Unfortunately, despite frequent amplification, overexpression or mutation of EGFR in glioblastomas, results were disappointing (Chakravarti et al., 2006; Haas-Kogan et al., 2005; Rich et al., 2004; Van Den Bent et al., 2007; Wen et al., 2006). Few patients have a clinical response to EGFR kinase inhibitors, and those who do respond initially, subsequently undergo rapid progression (Ziegler et al., 2008).
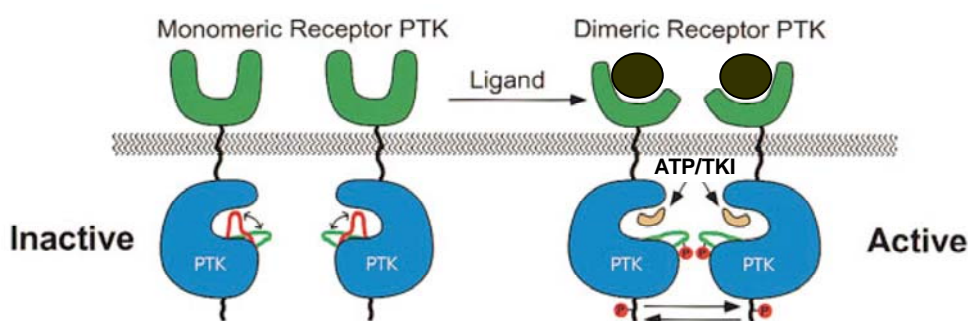
Figure 2.4. Model for the activation of the protein tyrosine kinase (PTK)-ErbB receptors, and their inhibition by small-molecule tyrosine kinase inhibitors (TKI). Ligand-induced receptor dimerization (2:2 ligand to receptor configuration) permits binding of ATP to the catalytic ATP binding pocket followed by trans-phosphorylation of additional tyrosine residues that serve as binding sites for downstream signalling proteins. Small-molecule tyrosine kinase inhibitors (TKI) compete with ATP in the ATP binding pocket, thereby inhibiting transphosphorylation and downstream signalling. Modified from Weiss and Schlessinger, 1998.

Agent (TKI)	GBM	Clinical trials in GBM
gefitinib (ZD-1839)	recurrent GBM	phase II (a)
	newly diagnosed GBM	phase II (b)*
erlotinib (OSI-774)	recurrent GBM	phase II (c)*
AEE788	recurrent GBM	phase I (d)*

Table 2.2. EGFR targeted therapies with small-molecule tyrosine kinase inhibitors (TKI) for glioblastoma (GBM) therapy.

a: (Rich et al., 2004); b: (Uhm et al., 2004); c: (Cloughesy et al., 2005; Raizer et al., 2004; Van Den Bent et al., 2007); d: (Baselga et al., 2005; Reardon et al., 2005). * Preliminary results presented in the form of abstract.

Mutations involving the ATP binding pocket of the tyrosine kinase domain of EGFR appear to be associated with response to EGFR-inhibition in non-small-cell lung cancer (Lynch et al., 2004; Paez et al., 2004). Consequently, mutant EGFR found in a subset of glioblastomas (EGFRvIII) – which has ligand-independent kinase activity – has been assessed for association with response to EGFR-targeted therapy. In spite of controversial in vitro studies, and one clinical study disclosing an association between responsiveness to EGFR-TKIs and co-expression of EGFRvIII and PTEN (Mellinghoff et al., 2005), no clear association could be found in other clinical settings (Haas-Kogan et al., 2005).

Thus, the reason for the relative resistance of glioblastoma to EGFR-targeted therapy using small-molecule tyrosine kinase inhibitors still remains an open question doubtlessly worth being adressed.

3.   Aim of the study

Glioblastoma (GBM) is a highly lethal malignant neoplasm that resists current therapies, which makes novel therapeutic options especially valuable. Even though *de novo* GBM is acknowledged to be highly dependent on EGFR signalling (Ohgaki et al., 2004), the promising EGFR-targeted therapy with small-molecule tyrosine kinase inhibitors (TKIs) showed up to date only disappointing effects in clinical settings (Chakravarti et al., 2006; Haas-Kogan et al., 2005; Rich et al., 2004; Van Den Bent et al., 2007).

The aim of the present study was therefore to elucidate additional receptor dependency of growth-inhibiting and radiosensitizing effects of EGFR-TKIs in a preclinical experimental setting. Furthermore, due to the propensity of ErbB2-receptors to act as "amplifiers" of EGFR signalling, it seemed most interestingly to evaluate the efficacy of additional ErbB2- receptor inhibition with bispecific EGFR/ErbB2 inhibitors.

Selection of the most appropriate model for investigation of EGFR and ErbB2 targeted therapy warranted thorough characterization of GBM cell lines according to their EGFR and ErbB2-receptor profiles and major downstream pathways. The most suitable cell lines with an inverse ratio of EGFR and ErbB2-receptor were selected and treated with specific EGFR or bispecific EGFR/ErbB2-receptor TKIs. Growth-inhibiting and radiosensitizing effects were correlated to cellular EGFR and ErbB2-receptor status.

Additionally, pathways downstream to ErbB receptors most probably responsible for the biological effects following receptor inhibition with EGFR TKIs and bispecific EGFR/ErbB2-receptor TKIs were investigated.

Keeping in mind the abundancy of intracellular signal transduction pathways downstream to the growth factor receptors, it was chosen to focus on the Akt and MAPK signalling pathways as they are widely recognized as the main signalling pathways downstream to EGFR and ErbB2-receptors (Yarden and Sliwkowski, 2001). Following EGFR or EGFR/ErbB2 TKI-treatment of the cells, Akt and MAPK activities were assessed by biochemical techniques. Furthermore, growth inhibition resulting from specific inhibition of the Akt and MAPK-pathway, respectively, was evaluated.

4.   Materials and Methods

4.1.   Materials

4.1.1. Reagents and Equipment

All chemical reagents used in the present work, and unless stated otherwise, were supplied by Carl Roth GmbH&Co. KG, Karlsruhe, Germany and Sigma-Aldrich, Irvine, United Kingdom. Cell culturing reagents as cell culture media (DMEM and RPMI 1640), fetal bovine serum (FBS), streptomycine, penicillin, glutamine and Trypsin/EDTA were obtained from Gibco-BRL, Karlsruhe, Germany. Reagents for the Bradford protein quantification assay were purchased from Bio-Rad Laboratories, Inc., Munich, Germany.

Protein A-Sepharose CL-4B was purchased from Amersham/Pharmacia Biotech, Freiburg, Germany. The chemiluminiscent visualization of proteins was performed using ECL Western blotting detection reagents obtained from Amersham/Pharmacia Biotech, Freiburg, Germany or SuperSignal® West chemoluminescent substrates from Pierce, Perbio Science, Bonn, Germany. Cyanin-5 (Cy5)-conjugated Streptavidin, used for FACS-analysis, was obtained from Jackson ImmunoResearch, Baltimore.

The Diff-Quik staining set used in the colony formation assay was from Medion Diagnostics AG, Düdingen, Switzerland.

Sterile cell culture plasticware was obtained from Sarstedt AG&Co, Nümbrecht, Germany. Immobilion-P polyvinylidene difluoride (PVDF) transfer membranes were purchased from Immobilion Millipore Corporation, Bedford, USA, and the autoradiography film Amersham Hyperfilm^{TM} ECL was supplied by Amersham/Pharmacia Biotech, Freiburg, Germany.

The humidified incubator Heraeus® cytoperm® 2 and the laminar flow workbench HERA-safe were purchased from Kendro and Heraeus-Instruments, Hanau, Germany. Cell counting was performed using the CASY® Model TT electronic cell counter obtained by Schärfe System, Reutlingen, Germany. The cytotoxicity assay was evaluated using the photometer Digiscan from ASYS Hitech GmbH, distributed by Mikrotek Laborsysteme GmbH, Hohenlinden, Germany. The spectrophotometer DU530 used for the Bradford protein quantification assay was obtained from Beckmann, Fullerton, CA, USA.

Equipment used for electrophoretic seperation and blotting of proteins was obtained from BioRad, Hercules, CA, USA (Mini-PROTEAN® 2-D electrophoresis cell, Trans-Blot® SD Semi-Dry Electrophoretic Transfer Cell, electrophoresis power supply Power Pac 300), Biometra, Göttingen, Germany (Multigel-Long electrophoresis cell, electrophresis power supply Power Pack 25) and Hoefer, San Francisco, USA (Transphor Electrophoretic Transfer Unit for wet blotting). Amersham Hyperprocessor™ Automatic Film Processor was purchased from Amersham, Braunschweig, Germany.

Cytometric analysis were performed using FACS Calibur flow cytometer from BD Biosciences, San Diego, CA, USA.

4.1.2. Buffers and solutions

- Amidoblack-destain solution: 10% methanol, 10% acetic acid, 80% A.d.
- Bradford-reagent: 0.01 % Coomassie Brilliant blue G-250, 4.7 % ethanol, 8.5 % phosphoric acid, A.d. ad 1 liter
- Crystal-violet staining solution: 0.04% crystal violet (N-hexamethylpararosaniline) in 4% (v/v) ethanol
- Cell Lysis buffer (standard): 20 mM Tris–HCl (pH 7.5), 150 mM NaCl,
  1 mM EDTA, 1 mM EGTA, 1 % Triton X-100,
  2.5 mM sodium pyrophosphate, 1 mM sodium orthovanadate, 1 mM β-glycerolphosphate,
  1 µg/ml leupeptin, 1 mM PMSF
- Cell Lysis buffer (IP): 10 mM Tris–HCl (pH 7.4), 130 mM NaCl,
  5 mM EDTA, 1% Triton X-100, 20 mM sodium phosphate (pH 7.5), 10 mM sodium pyrophosphate
  (pH 7.0), 50 mM NaF, 1 mM sodium orthovanadate,
  1 mM β-glycerolphosphate, and protease inhibitors
  (Roche Diagnostics, Mannheim, Germany)
- PBS buffer (pH 7.4): 138 mM NaCl, 4.3 nM Na_2PO_4, 1.4 mM KH_2PO_4
- SDS electrophoresis buffer: 25 mM Tris, 192 mM Glycin, 0.1 % SDS in A.d.

- SDS-gel solutions:
    - SDS resolving gel: 5-15 % Polyacrylamide, 375 mM Tris/HCl (pH 8.8), 0.1 % SDS, 0.3 % APS, 0.1 % TEMED
    - SDS stacking gel: 5 % Polyacrylamide, 12.5 mM Tris/HCl (pH 6.8), 0.1 % SDS, 0.3 % APS, 0.1 % TEMED
- SDS sample buffer: 62.5 mM Tris-Cl (pH 6.8), 2 % SDS, 10 % Glycerol, 50 mM DTT, 0.1 % Bromphenol blue (Tetrabromophenolsulfonephthalein)
- TBS buffer (pH 7.5): 20 mM Tris, 138 mM NaCl
- TPBS buffer (pH 7.4): 138 mM NaCl, 4.3 nM Na_2PO_4, 1.4 mM KH_2PO_4, 0.1 % Tween 20
- Transfer buffers (semi-dry blot):
    - Anode buffer I: 300 mM Tris, 20 % methanol in A.d.
    - Anode buffer II: 25 mM Tris, 20% methanol in A.d.
    - Cathode buffer: 25 mM Tris, 40 mM 6-Aminocapronic acid, 20 % methanol in A.d.
- Transfer buffer (wet-blot): 25 mM Tris, 192 mM glycin, 0.1 % SDS in A.d., 20 % Methanol in A.d.
- TTBS buffer: 20 mM Tris, 138 mM NaCl, 0.1 % Tween 20

4.1.3. Cells

The established human cancer cell lines LN-18, LN-229 and LN-Z308, derived from de novo human glioblastoma specimens, were a kind gift from Dr. E. von Meir, Lausanne, Switzerland. (Diserens et al., 1981; Ishii et al., 1999)

G-109, a cell line derived from a secondary human glioblastoma multiforme specimen, was obtained from K. Münkel and Dr. B. Eifert, Department of Neurosurgery, University of Heidelberg, Germany, where it was initially established. (Kraus et al., 2000; Kraus et al., 1999)

4.1.4. Activators and Inhibitors

Epidermal growth factor (EGF) was purchased from Upstate Biotechnology, NY, USA.

All tyrosine-kinase inhibitors used were reversible inhibitors competitive with ATP for the katalytic domain of the receptor protein tyrosine kinase.

Tyrphostin AG1478 [N-(3-Chlorophenyl)-6,7-dimethoxy-4-quinazolinamine] was obtained from Sigma-Aldrich, Irvine, United Kingdom. The amount of AG1478 required to inhibit enzyme activity by 50 % (IC_{50}) was shown to be 0.003 µM for EGFR and more than 100 µM for ErbB2 (Table 4.1.) (Levitzki and Gazit, 1995). Its high selectivity for EGFR disclosed in enzyme studies was confirmed in cell-based assays (Levitzki and Gazit, 1995).

The pyrrolo-pyrimidines PKI166 and AEE788 were a kind gift from Novartis Pharma AG, Basel, Switzerland. They represent two bispecific EGFR-/ErbB2-inhibitors, AEE788 being more potent with regard to ErbB2 inhibition (IC_{50}(PKI166) = 0.011µM, IC_{50}(AEE788) = 0.006µM) (Traxler et al., 2004; Traxler et al., 2001) (Table 4.1.).

The specific phosphatidylinositol 3-kinase (PI3-kinase) inhibitor LY294002 [2-(4-Morpholinyl)-8-phenyl-4H-1-benzopyran-4-one] represents a competitive inhibitor for the ATP-binding site of serine/threonine kinase PI3-kinase and does not inhibit other ATP-requiring enzymes (Vlahos et al., 1994). PD 98059 [2′-Amino-3′-methoxyflavone] was revealed to be a selective inhibitor of the MAP kinase activating enzyme MEK with no inhibitory activity against a number of other serine/threonine and tyrosine kinases (Dudley et al., 1995; Langlois et al., 1995; Pang et al., 1995). LY294002 and PD98059 were purchased from Calbiochem-Novabiochem, Schwalbach, Germany. Their selectivity for PI3-kinase (IC_{50}(LY294002) = 1.4 µM) or MEK (IC_{50}(PD98059) = 2 µM) was confirmed in whole-cell assays (Dudley et al., 1995; Vlahos et al., 1994) (Table 4.2.).

According to the manufacturer's specification, each compound was dissolved in dimethyl sulfoxide (DMSO) to make an initial stock solution and was stored at −20°C. During cell experiments final DMSO concentration remained less than 0.5%, with the exception of 25µM dilution of AG1478, where it reached 0.8%.

	Small-molecule Tyrosine-kinase-inhibitors		
Kinase	AG1478 IC_{50} (µM)	PKI166 IC_{50} (µM)	AEE788 IC_{50} (µM)
EGFR (ErbB1)	0.003 (a)	0.002 (b)	0.002 (c)
ErbB2	> 100 (a)	0.011 (b)	0.006 (c)
ErbB4		0.433 (b)	0.160 (c)

Table 4.1. In vitro profile of the small-molecule Tyrosine kinase inhibitors AG1478, PKI166 and AEE788 against ErbB-receptors. a: (Levitzki and Gazit, 1995); b: (Traxler et al., 2001); c: (Traxler et al., 2004).

	Inhibitors of MAPK and AKT signalling pathways	
Kinase	LY294002 IC_{50} (µM)	PD 98059 IC_{50} (µM)
PI3-kinase	1.4 (a)	> 100 (b)
MAPK kinase (MEK)	> 50 (a)	2 (c); < 10 (b)

Table 4.2. In vitro profile of LY294002, inhibitor of the Akt signalling pathway, and PD98059, inhibitor of the MAPK signalling pathway, against PI3-kinase and MAPK kinase (MEK). a: (Vlahos et al., 1994); b: (Dudley et al., 1995); c: (Pang et al., 1995).

4.1.5. Antibodies

The antibodies used in the present work are listed in table 4.3. All antibodies were stored and applied as recommended by the manufacturer.

In brief, anti-phospho-tyrosine (clone pY20) and all antibodies obtained from Cell Signalling Technology, Inc. were kept at –20°C. The remaining antibodies were stored at 2-8°C.

Biotinylated anti-EGFR and anti-ErbB2 antibodies were needed for flow cytometric experiments. Horseradish peroxidase–conjugated (HRP-linked) anti-rabbit and anti-mouse antibodies were used as secondary antibodies in chemiluminescent Western blotting applications. Those marked "IP" were used after immunoprecipitation only. All other experiments requiring HRP-linked antibodies were performed using the ones obtained from Cell Signalling Technology, Inc., Beverly, USA.

Antibody	Antigen	MW [kDa]	Dilution	Source	Company
Anti-EGFR	human EGFR (C-terminus)	170	1:1000 in 5% BSA in TPBS	polyclonal rabbit IgG	Santa Cruz Biotechnology, Inc., Santa Cruz, CA, USA
Anti-ErbB2	human c-erbB-2	185	1:500 in TTBS	polyclonal rabbit IgG	DakoCytomation, Glostrup, Denmark
biotinylated Anti-EGFR	human EGFR	170		monoclonal mouse IgG1	Cymbus Biotechnology Ltd., Hants, UK
biotinylated Anti-ErbB2	human c-erbB-2	185		monoclonal mouse IgG1	BioSource, Nivelles, Belgium
Anti-phospho-tyrosine, clone 4G10	phosphotyrosine		1:2000 in 5% BSA in TPBS	monoclonal mouse IgG$_{2b\kappa}$	Upstate Biotechnology, NY, USA
Anti-phospho-tyrosine, clone pY20	phosphotyrosine		1:2000 in 5% BSA in TPBS	monoclonal mouse IgG$_{2b}$	PharMingen, Heidelberg, Germany
Anti-mouse	Mouse Ig			polyclonal rabbit IgG+IgM	Jackson ImmunoResearch, Baltimore
Anti-Akt	human Akt (C-terminus)	60	1:1000 in TTBS	polyclonal rabbit IgG	Cell Signaling Technology, Inc., Beverly, USA
Anti-phospho-Akt (Ser473)	human Akt phosphorylated at Ser473	60	1:1000 in TTBS	polyclonal rabbit IgG	
Anti-p42/44 MAPK	Human p42/44 MAPK	42/44	1:1000 in TTBS	polyclonal rabbit IgG	
Anti-Phospho-p42/44 MAPK	Human p42/44 MAPK phosphorylated at Thr202/Thr204	42/44	1:1000 in TTBS	polyclonal rabbit IgG	
HRP-linked anti-mouse (IP)	mouse Ig		1:10000 in 5% BSA in TPBS	polyclonal sheep IgG	Amersham /Pharmacia Biotech, Freiburg, Germany
HRP-linked anti-rabbit (IP)	rabbit Ig		1:10000 in 5% BSA in TPBS	polyclonal donkey IgG	
HRP-linked anti-mouse	mouse Ig		1:2000 in 5% NFDM in TTBS	polyclonal horse IgG	Cell Signaling Technology, Inc., Beverly, USA
HRP-linked anti-rabbit	rabbit Ig		1:2000 in 5% NFDM in TTBS	polyclonal goat IgG	

Table 4.3. Antibodies used in the present work. (MW = molecular weight; NFDM = nonfat dried milk)

4.2. Methods

4.2.1. Cell cultivation

LN-18, LN-229 and LN-Z308 cell lines were maintained in Dulbecco's modified Eagle medium (DMEM) supplemented with 100 U/ml penicillin, 100μg/ml streptomycin, 1% L-glutamate and 10 % fetal bovine serum (FBS). G-109 cells were maintained in equally supplemented RPMI 1640 medium. All cell lines were grown as monolayer cultures in 100mm petri dishes under standard conditions in a 92% humidified incubator containing 5% CO_2 at 37°C and medium was changed at a regular basis every 2-3 days. At reaching 80% confluency cells were either passaged for subcultivation or plated for experiments.

For cryoconservation cells were detached with trypsin, centrifuged (1500 rpm, 2 min), resuspended in 1ml DMEM supplemented with 100 U/ml penicillin, 10μg/ml streptomycin, 1% L-glutamate, 20% FBS and 5% DMSO and finally stored at –80°C.

To assure genetic integrity cells maintained in culture were replaced from an initially generated cryoconserved stock every 4-6 weeks.

4.2.2. Pretreatment of cells

For protein extraction prior to western blotting of whole cell lysates cell stocks were grown to 80% confluence, trypsinized, plated at 9.5×10^4 cells per well on 6-well plates and incubated for 24 hours under standard conditions. Following 12 hours deprivation from FBS cells were treated with inhibitors in desired concentrations for 1 hour. 10ng/ml EGF was added for 5 minutes and cells were lysed as described below (chapter 4.2.4.1.).

Modifications applied prior to EGFR-Immunoprecipitation included a plating density of 8×10^5 cells per 100mm Petri dish and 24 hours deprivation from FBS. Cells were treated in duplicate with 1μM and 10μM AEE788 for 30 minutes before addition of EGF and cell lysis.

For cytotoxicity- and colony formation assays cell stocks were grown to 80% confluence, trypsinized, plated into 24-well-tissue culture plates at 2×10^4 cells/well and allowed to attach by 24 hour incubation under standard conditions. Treatment with inhibitors (listed in chapter 4.1.5.) was performed as a single administration of the compounds in equimolar concentrations of 0.1, 1, 5, 10 and 25μM. Following 12 hour incubation, cells were irradiated as described below (chapter 4.2.3.), and replaced into the incubator immediately after.

36 hours later and in total 48 hours after inhibitor-treatment cells were either transferred to 6-well-dishes for clonogenic evaluation (chapter 4.2.7.), or fixed and stained for immediate assessment of cytotoxic injury as described below (chapter 4.2.6.). For kinetic evaluation of cytotoxicity incubation was terminated 6, 12, 18, 24, 36 and 48 hours after treatment with inhibitors.

4.2.3. Irradiation

All irradiation procedures were conducted at the Department of Radiation Oncology, Klinikum Rechts der Isar, Technical University Munich (Director: Prof. Dr. med. M. Molls). Cells were gamma-irradiated at room temperature with single doses of 2, 4, 6, 8 or 10Gy using a cobald ^{60}Co source (6MeV) at a dose rate of 6 Gy/min. Standard cell conditions were maintained by performing a change of medium, with or without inhibitors, 12 hours before treatment and irradiating at a set time, to avoid the effects of diurnal variation. Control probes were brought to the irradiation department and handled likewise.

4.2.4. Protein biochemistry techniques

4.2.4.1.   Protein extraction

According to standard protocols, cells were washed with PBS, incubated for 15 minutes in 150μl standard-lysis buffer per 35mm well, scraped off the dish and transferred to 1.5 ml eppendorf tubes. Cell debris was removed by centrifugation (10000rpm, 15min, 4°C) and the supernatant either quantified and subjected to SDS-polyacrylamide gel electrophoresis immediately after (chapter 4.2.4.2. and 4.2.4.4.) or stored at −80°C.

For protein extraction prior to immunoprecipitation cells were washed with PBS, shortly incubated with 1ml IP-lysis buffer per 100mm cell dish, scraped off the dish and transferred to 1.5 ml eppendorf tubes. They were incubated rotating at 4°C for 20 minutes and clarified by centrifugation (13000rpm, 5 min, 4°C). Immunoprecipitation as described below (chapter 4.2.4.2.) followed immediately after.

To avoid proteolysis, dephosphorylation and denaturation, all steps were strictly performed on ice using only ice-cold reagents and pre-cooled equipment.

4.2.4.2. Bradford protein quantification assay

Total protein concentration in the whole cell lysates was measured using the bradford-reagent (chapter 4.1.2.). Cell lysates were diluted 1:250 and 1:500 with 1xPBS and 1xPBS with 0.01% Triton X-100 respectively. Protein standard solutions containing 0-8µg/ml BSA in 0.01% TritonX-100/PBS were generated and Bradford-reagent was added to all test cuvettes. The assay is based on the ability of proteins to bind Coomassie brilliant blue G-250 and thereby cause a shift in the absorption maximum of the dye from 465nm to 595nm. The increase in absorption at 595nm is proportional to the protein concentration (Bradford, 1976). Based on this, absorption was measured at 595nm 30 minutes after addition of bradford-reagent and protein concentration of the cell lysates was counted by means of comparison with the previously generated standard solutions.

4.2.4.3. Immunoprecipitation

Immunoprecipitation was used to isolate EGFR-protein from whole cell lysates. The method is based on the specific binding of an antibody to the antigen of the targeted protein. Precipitation is finaly accomplished through binding of the antibody-protein-conjugate to Sepharose-bound Protein-A (protein A-beads) and subsequent isolation by centrifugation due to the high molecular weight of Sepharose.

Cells were treated and protein extracted as described above (chapter 4.2.2. and 4.2.4.1.). After centrifugation, 5 µl anti-EGFR antibody was added to the supernatant and incubated rotating overnight at 4°C. Addition of anti-mouse antibody to one probe served as negative control for unspecific binding. Subsequently, 25 µl precleared protein A-Sepharose was added to each test tube, incubated rotating for 1.5 hours at 4°C and centrifuged for 2 minutes at 14000rpm and 4°C. The pellet containing the precipitated protein A-Sepharose bound antibody-protein complexes was washed 3 times with 1ml cell lysis buffer (chapter 4.1.2.) and boiled with 25µl SDS-sample buffer for 10 minutes at 95°C to assure separation from protein A-beads and denaturation of the protein. After short centrifugation the supernatant was subjected to SDS-polyacrylamide gel electrophoresis.

Whole cell lysates of each precipitated probe served as control.

4.2.4.4.   SDS-polyacrylamide gel electrophoresis (SDS-PAGE)

Modified from the original method devised by Ornstein (Ornstein, 1964) and Davis (Davis, 1964), the procedure of discontinuous electrophoresis enables separation of protein mixtures according to size by sieving.

Minigels and Maxigels were cast varying the pore size of the resolving gel through different content of Polyacrylamide (5-15%; chapter 4.1.2.). After polimerization the plates were mounted in the electrophoresis apparatus and submerged in SDS electrophoresis buffer.

The pace of proteins in the electric field depending save from size from their form and electric charge, SDS-sample buffer was added to the protein lysates and to a marker of known molecular weight and the mixtures cooked for 5-10 minutes for denaturation before being loaded onto the gel. The anionic detergent SDS inherent in all PAGE-buffers assured a constant netto charge per mass unit (Laemmli, 1970).

Separation was performed at a constant electric current of 100-150 V for 1 – 3 hours.

4.2.4.5.   Immunoblotting

Electrophoretic transfer of proteins separated by SDS-PAGE onto the surface of an immobilizing PVDF-membrane was performed by Wet- or Semi-dry electroblotting. Wet – electroblotting, being generally preferable for transfer of heavy proteins, was used for the immunoprecipitated EGFR.

4.2.4.5.1.   Wet-electroblotting

The hydrophobic PVDF membrane was to be rinsed shortly in 100% methanol before being placed in electrode buffer. The gel and the membrane were assembled between two sheets of Whatman-paper avoiding air-bubbles. The stack was then placed between two foam pads and mounted in the transfer tank with the PVDF-membrane facing the anode. Transfer of EGFR was performed at a constant electric current of 1500mA for 90 minutes.

4.2.4.5.2.   Semi-dry electroblotting

For Semi-dry electroblotting a discontinuous buffer system was applied. The blotting stack consisted from anode to catode of 6 sheets of Whatman-paper soaked in anode buffer I, 3

sheets of Whatman-paper soaked in anode buffer II, the PVDF-membrane followed by the gel and 9 sheets of Whatman-paper soaked in cathode buffer. Transfer was performed at a constant electric current of 225 mA. Transfer time varied according to protein size.

4.2.4.5.3.   Immunochemical detection of protein

The membrane was incubated ("blocked") in 5% non-fat dried milk in TTBS or 5% BSA in TPBS at 37°C for 30 minutes to saturate unspecific binding sites, i.e. diminish unspecific background signal. After short rinsing in TTBS or TPBS respectively it was incubated in diluted primary antibody targeting the protein sought-after (for dilution see chapter 4.1.4.) rotating at 4°C over night. The membrane was washed with TTBS or TPBS respectively three times for 5-10 minutes, probed with diluted Horseradish peroxidise-conjugated secondary antibody targeting the Fc-region on the primary antibody (for dilution see chapter 4.1.4.) for 1 hour at room temperature and finally washed again 3 times for 5-10 minutes. For detection the membrane was incubated with chemiluminescent substrates (chapter 4.1.1.) resulting in light emission triggered by horseradish peroxidase. The chemiluminescent reaction was visualized by exposure to autoradiography films. Blots were scanned and quantification of protein expression performed by band analysis using ImageJ software 1.37v (developed at the U.S. National Institutes of Health and available on the Internet at http://rsb.info.nih.gov/ij/).

If the same membrane was desired to be re-probed for a further protein, the initially used antibody had to be detached first (i.e. stripped from the membrane). This was achieved by incubation with amidoblack-destain solution (chapter 4.1.2.) for 15 minutes at room temperature followed by thorough rinsing with deionized water.
Thereafter the membrane was re-blocked and re-probed for the desired protein as described above.

4.2.5. FACS-Analysis

Flow cytometric analysis of EGFR and ErbB2 expression levels were kindly performed in the Institute of Pathology, University of Regensburg, Germany (Director: Prof. Dr. med. F. Hofstädter).
Immunofluorescent staining was done with a two-step labeling technique as described before (Brockhoff et al., 2001). In short, cell stocks were grown to 80 % confluence, trypsinized, and

the cell suspension was adjusted to 10^6 cells/ml. Cells were incubated with 5 µg/ml biotinylated anti-EGFR or 5 µg/ml biotinylated anti-ErbB2-receptor antibody (chapter 4.1.5.) for 30 minutes, then washed with PBS followed by addition of 1 µM/ml Cyanin-5 (Cy5)-conjugated Streptavidin. After repeated washing with PBS the flow cytometric measurements were conducted using FACS-Calibur flow cytometer. Thereby a diode laser specifically excited the receptor-bound fluorescent marker Cy5 at 635 nm, and Cy5 emission was detected using a 661/16 nm band pass filter followed by the FL4 photomultiplier sensor, converting light emission in electrical pulses. Those were processed by an analog-to-digital-converter (ADC) which in turn allowed for the events to be plotted on a graphical scale. The mean fluorescense intensity was calculated for each cell-line.

4.2.6. Cytotoxicity assay

Assessment of cytotoxicity by cell quantification using crystal violet staining was based on the method of Gillies (Gillies et al., 1986) and Saotome (Saotome et al., 1989).

Cells were plated onto 24-well-plates at $2x10^4$ cells/well and treated with inhibitors, irradiated and cultivated as described above (chapter 4.2.2.). The following steps were performed at room temperature. Medium was carefully removed, and cells were fixed with 4% formaldehyde in PBS for 30 minutes. After air-drying the wells for 5 minutes they were washed twice with PBS containing 0.1% Triton X-100 and twice with deionized water. Cells were stained with 500µl crystal-violet solution (chapter 4.1.2.) per well for 30 minutes and subsequently washed three times with deionized water. In order to solubilize the nucleoprotein-bound crystal violet 500µl 1% SDS solution was added to each well and incubated on a shaker for 1 hour. Complete solubility was confirmed under the microscope. Finally, the solution was transferred to 96-well plates (100µl/well) and absorbance was measured at 570 nm.

For evaluation of cytotoxicity either the absorbance measurment values were plotted directly as arbitrary units, or cell growth in each well calculated as the percentage of the average absorbance of the untreated control.

4.2.7. Colony formation assay

The proliferative potential of cells exposed to treatment was measured assessing their colony formation ability based on the method introduced by Puck (Puck and Marcus, 1956).

Cells were plated into 24-well-plates at $2x10^4$ cells/well and treated with inhibitors, irradiated and cultivated as described above (chapter 4.2.2.). 48 hours after inhibitor-treatment, cells were harvested, diluted 1:200 and plated for clonogenic survival into 6-well-plates. Medium was changed on day 3 and 6 and the assay terminated after 10 days incubation under standard conditions. Cells were fixed in Diff-Quik fixative solution (50%methanol) for 10 minutes. Following staining with 1ml Diff-Quik solution I /II for 30 seconds each, dishes were rinsed three times with deionized water to remove excess dye and air-dried overnight. A flat bed scanner was used to aquire RGB color images of the culture dishes with a resolution of 300 pixels per inch (ppi), which were converted to grey-scale images to enabel further analysis. Subsequent automated counting of colonies by image analysis was based on the method of Dahle et al. (Dahle et al., 2004) and was kindly performed by E. Mannweiler, Institute of Pathology, Helmholtz Zentrum München, Neuherberg. Colonies consisting of more than 50 cells were counted. The surviving fraction was calculated as the percentage of colonies relative to controls.

4.2.8. Statistical analysis

A Pearson's linear correlation analysis was performed to compare direct cell count with the absorbance of crystal violet stained cells using SPSS software version 15 (SPSS Inc, Chicago, IL).

Statistical analysis of the dose-dependent effects of inhibitors on cell survival as measured with the crystal violet cytotoxicity assay was performed with one-way analysis of variance (ANOVA) followed by Bonferroni post-hoc testing. Differences between growth-inhibiting efficacys of inhibitors and differences of cell-survival with respect to dosage and incubation time were evaluated using two-way ANOVA followed by Bonferroni post-hoc testing. In both cases Graph Pad Prism software, version 5 (GraphPad Software Inc, La Jolla, CA) was used.

Surviving fractions determined with the colony formation assay were fitted into the classical linear-quadratic equation, $S = \exp(-\alpha D - \beta D^2)$, where S is the surviving fraction, D the radiation dose and α and β adjustable parameters. The 95% confidence band was plotted for each survival curve. Calculations were made through nonlinear least-squares regression, using Graph Pad Prism software, version 5 (GraphPad Software Inc, La Jolla, CA).

5.   Results

5.1.   The bispecific EGFR/ErbB2-receptor tyrosine kinase inhibitor AEE778 shows a strong inhibiting effect on EGFR- and ErbB2-activation in glioma cell lines.

As shown by earlier studies, the small-molecule tyrosine kinase inhibitor AEE788 acts as a bispecific inhibitor of the EGFR and ErbB2-receptor. In the present study the effect of AEE788 on EGFR/ErbB2-receptor signalling was assessed in the special case of glioma cells. Representative serum-starved LN-18 cells were treated with 1 and 10 µM AEE788 for 30 minutes before addition of 10 ng/ml EGF and subsequent cell-lysis. After immuno-precipitation of EGFR, its activated (i.e. phosphorylated) state was visualized by strong phospho-tyrosine immunoreactivity (Fig. 5.1., upper panel, line 2). The potency of AEE788 to block EGFR-activation was shown by an absent phospho-tyrosine immunoreactivity after treatment with 10 µM and even 1 µM AEE788 (Fig. 5.1., upper panel, line 4 and 3), though the presence of EGFR in the lysat was clearly demonstrated (Fig. 5.1., middle panel, line 1-4).
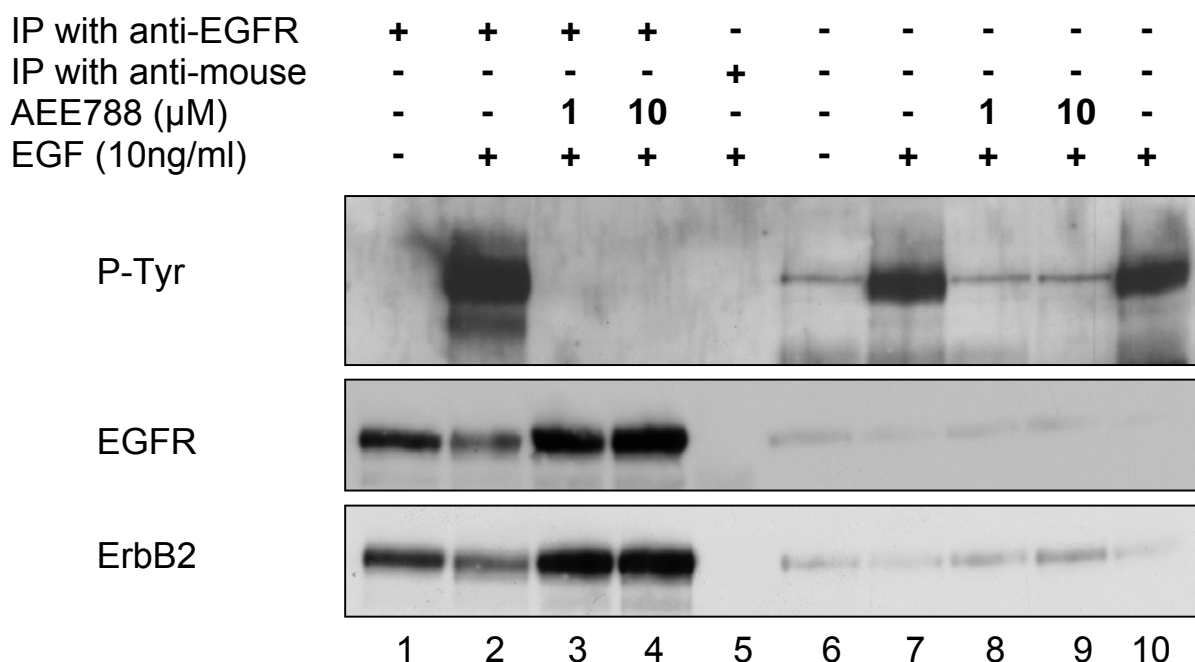
Figure 5.1. Phosphorylation pattern of EGFR and ErbB2-receptor after immunprecipitation (IP) of EGFR as revealed by immunoblotting (upper panel). LN-18 cells were treated with AEE788 (1 µM, 10 µM) and epidermal growth factor (EGF, 10 ng/ml) as indicated. SDS-gels were loaded in dublicate, each probed for phospho-tyrosine (p-Tyr; upper panel), stripped and subsequently probed for EGFR (middle panel) and ErbB2 (lower panel) respectively. Protein-lysates immunoprecipitated with anti-mouse antibody (line 5) and non-immunoprecipitated whole cell lysates (line 6 to 10) served as control.

Most interestingly, ErbB2-receptor was shown to co-immunoprecipitate with EGFR (Fig. 5.1., lower panel, line 1-4). And it should be noted, that the immunoreaction for both EGFR and ErbB2 was weakest for the activated non-inhibited receptors (Fig. 5.1., middle and lower panel, line 2), indicating a lower number of receptor compared to the non-activated state. The strongest immunoreaction for EGFR and ErbB2, indicating the highest quantity of receptor, was detectable with inhibition of the activated receptor (Fig. 5.1., middle and lower panel, line 3 and 4).

5.2. Glioma cell lines co-express high levels of EGFR and ErbB2 oncoprotein

Because the relative expression of ErbB receptors has been shown to change depending on culture conditions (Gulliford et al., 1997), a quantitative expression profile of EGFR and ErbB2-receptor was performed for the experimental conditions of the present study in four glioma cell lines. It was performed using FACS-analysis.

Cell lines with high expression of EGFR and comparably low expression of ErbB2 included LN-308 and LN-18. Both G-109 and LN-229 showed high expression of ErbB2 and comparably low expression of EGFR (Fig. 5.2.).
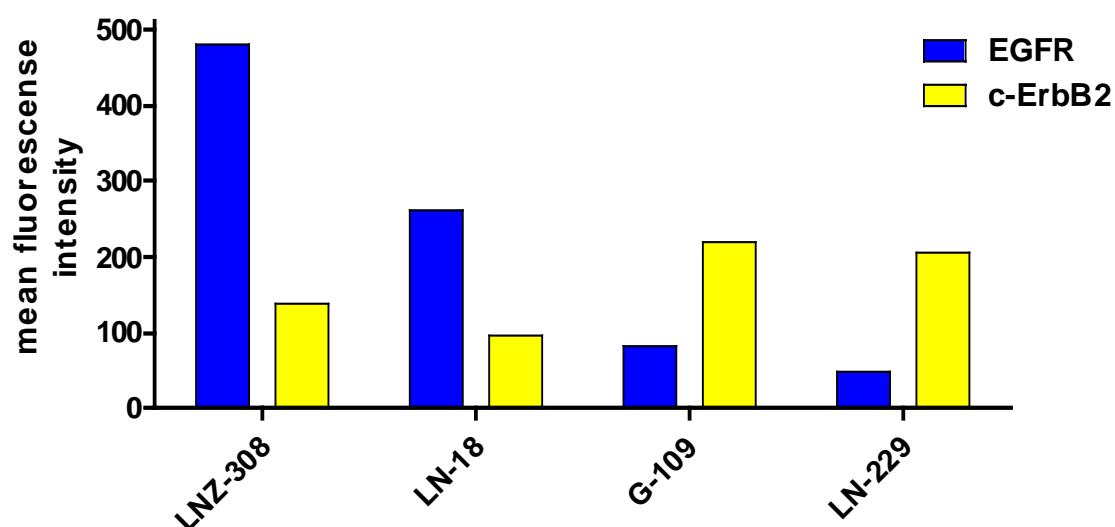
Figure 5.2. Quantitative expression of EGFR and ErbB-2 detected by FACS-analysis in human glioma cell lines LNZ-308, LN-18, G-109 and LN-229. Data are presented as background corrected mean fluorescense intensity.

5.3. LN-18 and LN-229 cells are a suitable model for investigation of EGFR and ErbB2-receptor signalling inhibition in glioma cells

In order to choose the most suitable model for the investigation of EGFR/ErbB2-receptor inhibition, the cell lines were further characterized according to original tumor, the two major pathways downstream to the EGFR/ErbB2-receptors and p53 protein expression. (Table 5.1.) All cell lines derived from *de novo* GBM, with the exception of G-109 which originated from secondary GBM. Previous work by our laboratory and others revealed constitutively activated Akt in LNZ-308, LN-18 and G-109 cells, which coincided with a mutation of the tumor suppression gene PTEN in LNZ-308 and G-109 cell lines, and constitutively activated MAPK in G-109 and LN-229 cells (Ishii et al., 1999; Kraus et al., 2000; Kraus et al., 1999; Schlegel et al., 2000). P53 protein expression was equally strong in LN-18 and LN-229 cells, weak in G-109 and absent in LNZ-308 cell lines (Kraus et al., 1999).

	LNZ-308	LN-18	G-109	LN-229
Original tumor	de novo GBM (a)	de novo GBM (a)	secondary GBM (d)	de novo GBM (a)
Akt	constitutively activated (c)	constitutively activated (c)	constitutively activated (c)	not activated (c)
PTEN	mutated (a)	wt (a)	mutated	wt (a)
MAPK	Not activated (c)	not activated (c)	constitutively activated (c)	constitutively activated (c)
p53 protein expression	- (b)	+++ (b)	+ (b)	+++ (b)

Table 5.1. Characterization of the GBM cell lines LNZ-308, LN-18, G-109 and LN-229 according to original tumor, Akt, PTEN, MAPK and p53 protein expression. a:(Ishii et al., 1999), b:(Kraus et al., 1999), c:(Schlegel et al., 2000), d:(Kraus et al., 2000)

On the basis of the FACS-data and further characterization listed in Table 5.1. LN-18 and LN-229 glioma cell lines were chosen for the present analysis. They represent two cell lines with an inverse ratio of EGFR and ErbB2-receptor respectively, which originate from *de novo* GBM specimens.

Their EGFR and ErbB2 status was confirmed using immunoblotting. The results confirmed the FACS-data showing a strong immunoreactivity for EGFR and weak immunoreactivity for ErbB2 in LN-18 cells (EGFR+++/ErbB2+). LN-229 cells presented a vice versa pattern with weak immunoreactivity for EGFR and strong immunoreactivity for ErbB2 (EGFR+/ErbB2+++) (Fig. 5.3.).
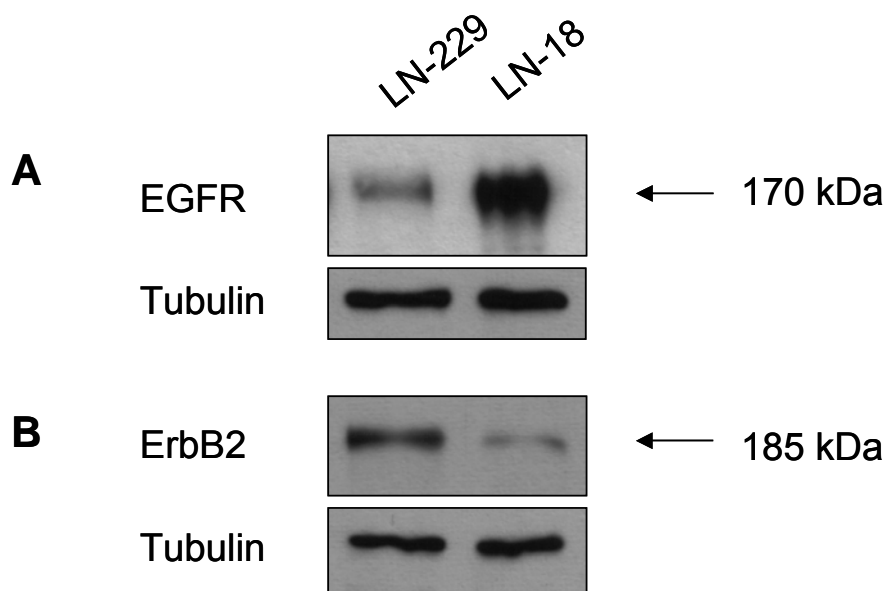
Figure 5.3. Total EGFR (A) and ErbB2 expression (B) detected by immunoblotting in human glioma cell lines LN-18 and LN-229 (5 µg total protein per lane). To ensure equivalent loading and transfer a tubulin-control was conducted (lower panel in A and B).

5.4. Cell number and absorbance after staining with crystal violet show a linear relationship in LN-18 and LN-229 glioma cells

To confirm the reliability of the crystal violet staining cytotoxicity test the absorbance of stained cells was plotted against the cell number in each corresponding well. A clear linear relationship for both cell lines LN-18 and LN-229 was confirmed (p < 0.0001), indicating that the absorbance corresponded to cell number within the range of cell numbers tested (Fig. 5.4.).
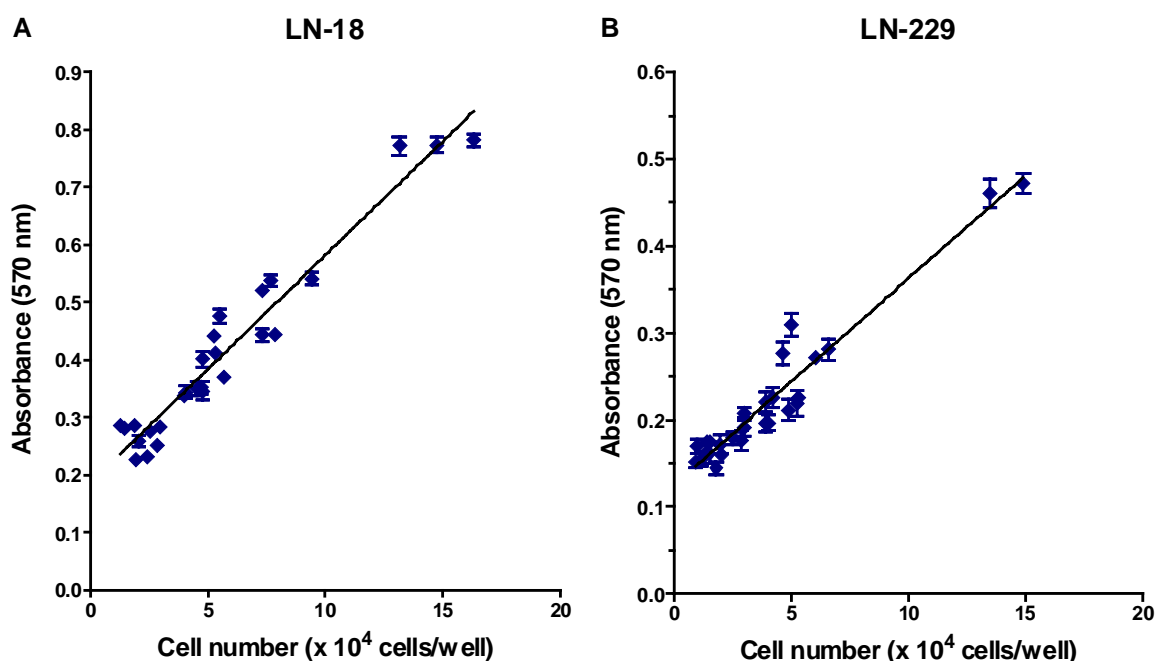
Figure 5.4. Linear relationship between direct cell count and absorbance of crystal violet stained (A) LN-18 and (B) LN-229 cells. LN-18 and LN-229 cells were incubated for up to 52 hours, stained with crystal violet and counted using the CASY® Model TT electronic cell counter. Linearity was confirmed with Pearson's linear correlation analysis (p < 0.0001). R^2 (LN-18) = 0.94; R^2 (LN-229) = 0.93. Error bars represent the 95% Confidence Interval of four replicate values.

5.5. EGFR-specific (AG1478) and bispecific EGFR/ErbB2-receptor inhibition (PKI166/AEE788) act differently on cell survival of LN-18 and LN-229 GBM cells

LN-18 cells (EGFR+++/ErbB2+) and LN-229 cells (EGFR+/ErbB2+++) were subjected to specific EGFR-inhibition with AG1478 or bispecific EGFR/ErbB2-receptor inhibition with PKI166 and AEE788 respectively. Cells were incubated with the indicated doses of inhibitors and the assay terminated 48 hours later by staining with crystal violet as described above (chapter 4.2.2. and 4.2.6.).

The three TKI showed different effects in the cell lines examined.

(a) In LN-18 cells the dosage needed to significantly decrease the surviving fraction varied with respect to the inhibitor, being 10 µM AG1478 (Fig. 5.5. A), 5 µM PKI166 and 1 µM AEE788 (Fig. 5.6. A and C). It should be noted that more efficent growth inhibition of LN-18 cells at low concentrations could only be achieved by additional blockage of ErbB2-receptors with bispecific TKIs – and among those AEE788 proved more efficient than PKI166, indicating a correlation with intrinsic potency of ErbB2 blockage.

(b) In LN-229 cells the dose needed for significant growth inhibition did not vary with EGFR- or bispecific EGFR/ErbB2-inhibition. Inhibition with AG1478 and AEE788 showed a quite similar pattern where only 0.1µM of the compounds were needed to result in significant
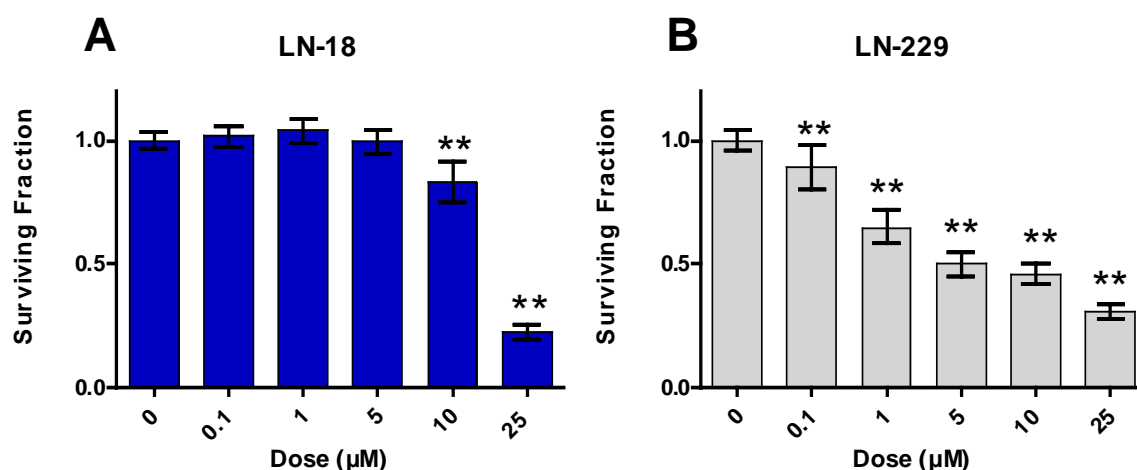
Figure 5.5. Effect of EGFR-specific Inhibitor AG1478 on LN-18 and LN-229 GBM cell lines. Cells were incubated with AG1478 for 48 hours, stained with crystal violet, the absorbance measured at 570 nm and the surviving fraction calculated as percentage of control cell growth (0µM AG1478). Error bars represent the standard deviation of at least 24 replicate values. Asterixes indicate the significance of the difference to control as determined using one-way ANOVA with Bonferroni post-hoc test (** $p < 0.001$).

growth inhibition and no difference could be disclosed between surviving fraction at 1 µM versus 5 µM of each substance (Fig. 5.5. B; Fig. 5.6. D).

Furthermore, LN-18 cells seemed to gain a growth stimulus at very low doses of 0.1µM of all inhibitors, though the difference failed to show statistical significance to the untreated control (Fig. 5.5.A; Fig. 5.6. A and C).
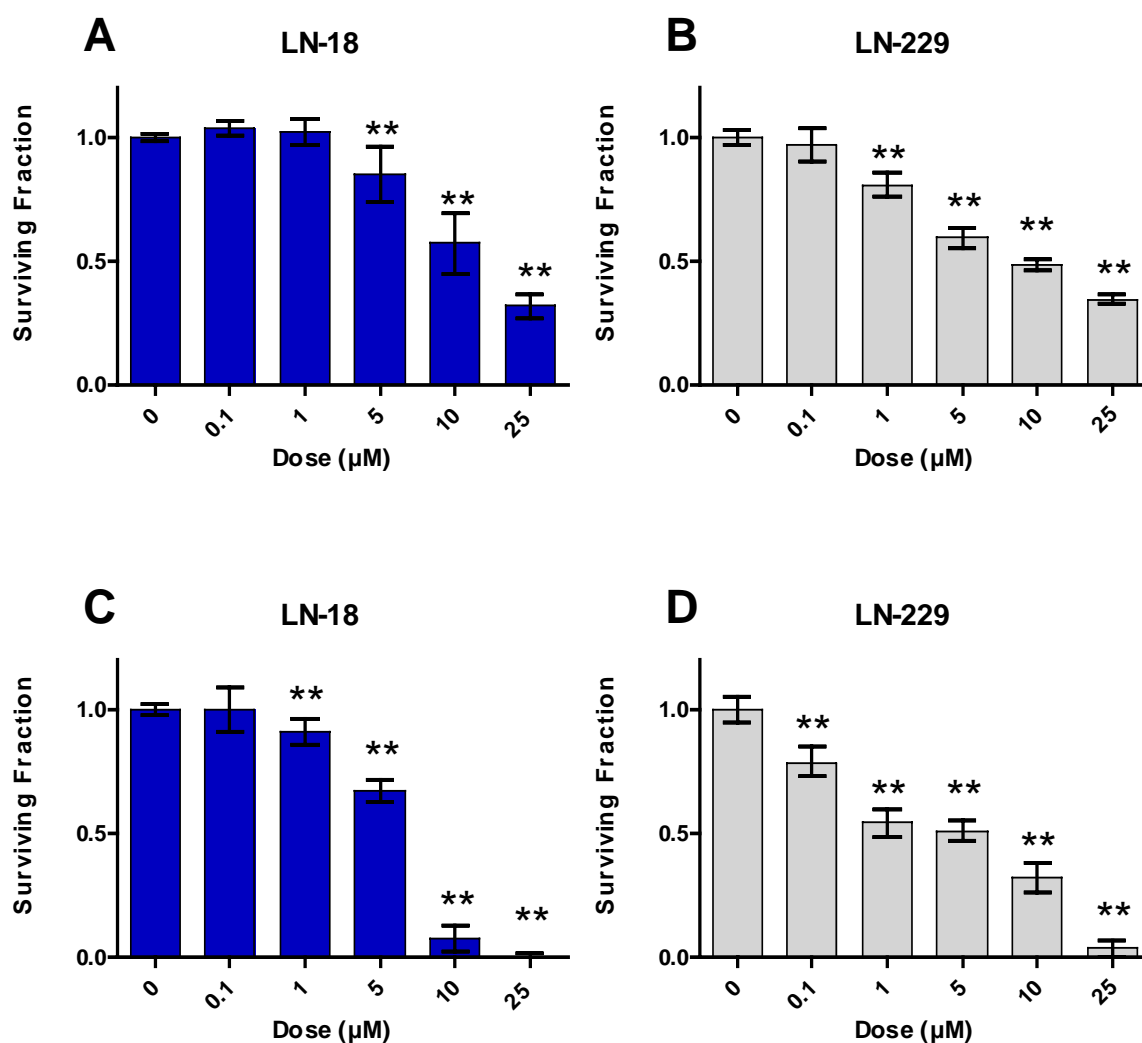
Figure 5.6. Effect of bispecific EGFR/ErbB2-Inhibitors (A, B) PKI166 and (C, D) AEE788 on LN-18 and LN-229 GBM cell lines. Cells were incubated with PKI166 or AEE788 for 48 hours, stained with crystal violet, the absorbance measured at 570 nm and the surviving fraction calculated as percentage of control cell growth (0µM PKI166/AEE788). Error bars represent the standard deviation of at least 24 replicate values. Asterixes indicate the significance of the difference to control as determined using one-way ANOVA with Bonferroni post-hoc test (** $p < 0.001$).

5.5.1. AEE788 acts more efficiently than PKI166 on growth-inhibition of both LN-18 and LN-229 GBM cells

Both bispecific TKIs AEE788 and PKI166 had growth inhibiting effects on LN-18 and LN-229 cells (Fig. 5.6.). To evaluate the difference of their respective efficacy, cells were incubated with the inhibitors and the surviving fraction evaluated as described above (chapter 5.5., chapter 4.2.2. and 4.2.6.).

AEE788 proved to have a clearly stronger impact on growth inhibition of both cell lines than achieved by PKI166, starting at a dose of 1 µM for LN-18 cells ($p < 0.001$) and 0.1 µM for LN-229 cells ($p < 0.001$) (Fig. 5.7.).
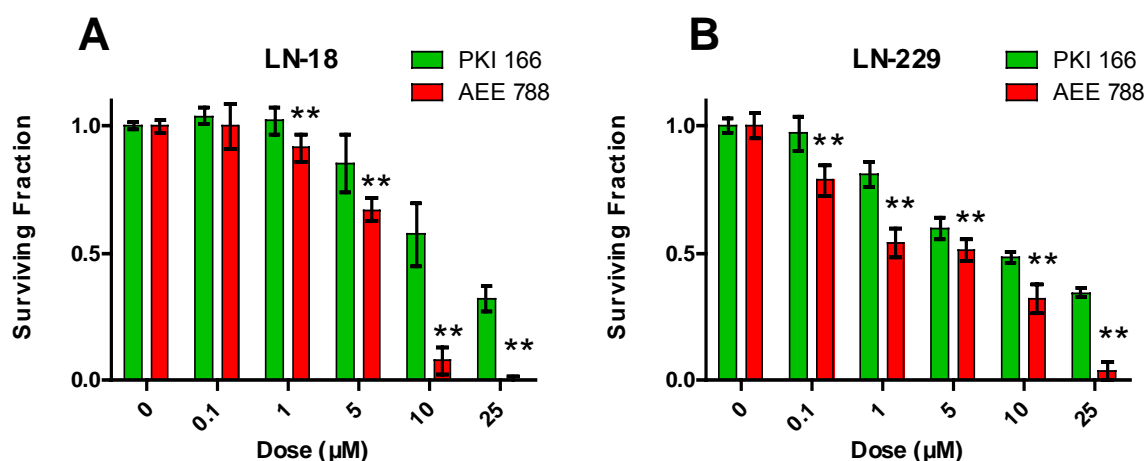
Figure 5.7. Higher efficacy of AEE788 versus PKI166 on growth inhibition of both (A) LN-18 and (B) LN-229 glioma cells. Cells were incubated with PKI166 or AEE788 for 48 hours, stained with crystal violet, the absorbance measured at 570 nm and the surviving fraction calculated as percentage of control cell growth (0µM PKI166/AEE788). Error bars represent the standard deviation of at least 24 replicate values. Asterixes indicate the significance of the difference in growth inhibition of corresponding doses of AEE788 versus PKI166 as determined with two-way ANOVA and Bonferroni post-hoc test (** $p < 0.001$).
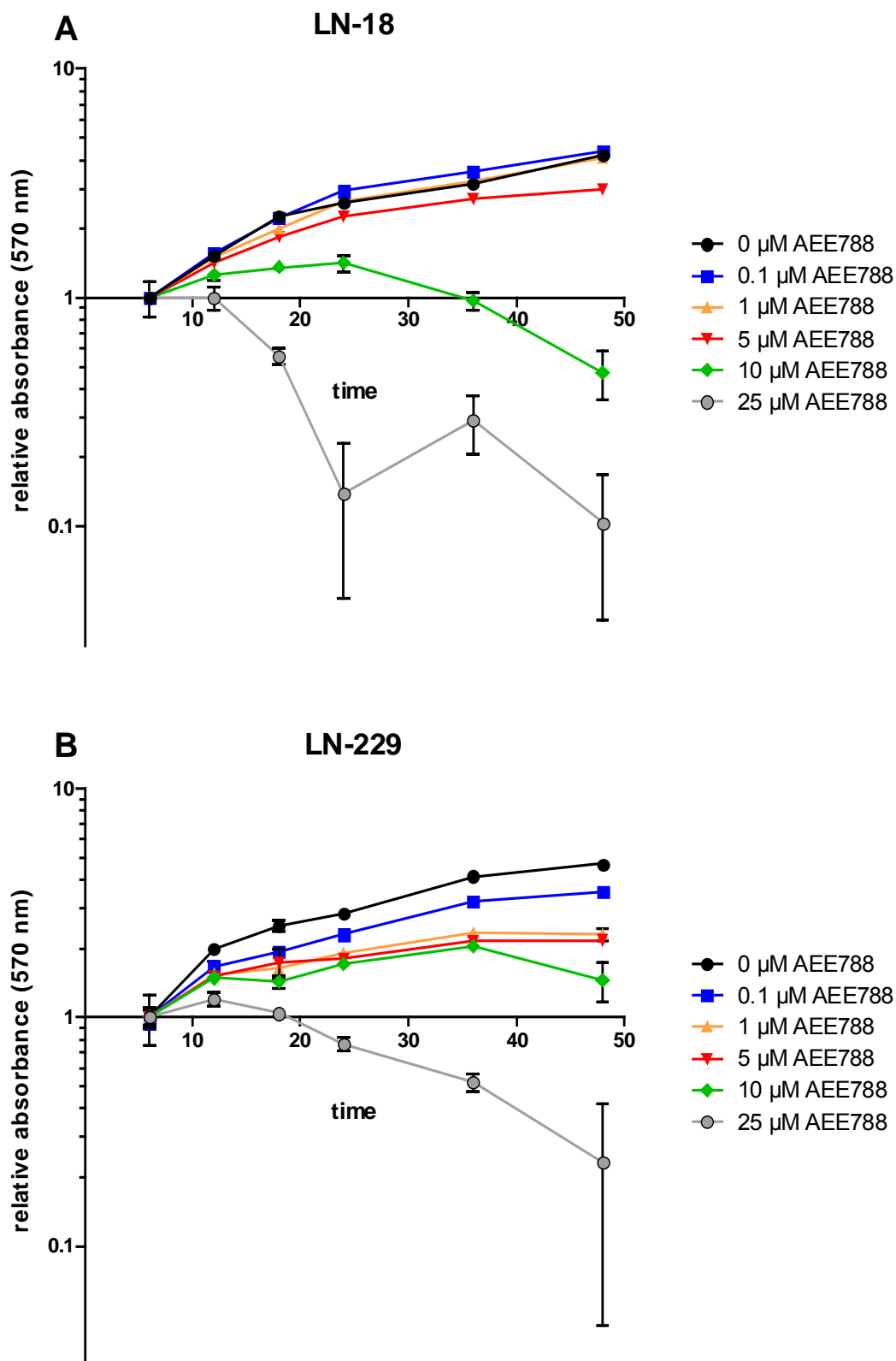
Figure 5.8. Dose dependent effect of AEE788 on (A) LN-18 and (B) LN-229 glioma cells. Cells were treated with increasing concentrations of AEE788 as indicated and growth inhibition evaluated 6, 12, 18, 24, 36 and 48 hours after. Data points represent the absorbance relative to the value 6 hours after treatment. Error bars depict the standard deviation of eight replicate values.

5.5.2. The bispecific EGFR/ErbB2-receptor tyrosine kinase inhibitor AEE788 has a dose-dependent effect on both LN-18 and LN-229 glioma cells

Kinetic experiments were conducted for further confirmation of growth inhibiting effects of AEE788. LN-18 and LN-229 cells were treated with increasing concentrations of AEE788 (0.1 to 25 µM) and growth inhibition was evaluated 6, 12, 18, 24, 36 and 48 hours after, as described above (chapter 4.2.2. and 4.2.6.).

A growth-stimulating effect of 0.1 µM AEE788 on LN-18 cells was observed commencing at 24 hours after incubation ($p < 0.001$ at 24, 36 and 48 hours). Growth-inhibition of LN-18 cells induced by 1 µM AEE788 could be assessed at 48 hours treatment only ($p < 0.001$). 5 µM AEE788 exerted a marked growth-inhibiting effect on LN-18 cells ($p < 0.05$ at 12 hours, $p < 0.001$ at 18-48 hours) (Fig. 5.8. A). In LN-229 cells all dosages of AEE788 resulted in marked growth inhibition compared to untreated control even after 12 hour incubation ($p < 0.001$ at 12, 18, 24, 36 and 48 hours). There was no significant difference in the effect of 1 µM versus 5 µM of AEE788 in LN-229 cells (Fig. 5.8. B). 10 µM and 25 µM AEE788 were shown to have exceedingly strong cytotoxic effects in both LN-18 and LN-229 cells (Fig. 5.8.). In conclusion, 5 µM AEE788 exerted marked, yet not overshooting growth-inhibiting effects on both cell lines as compared to untreated controls (Fig. 5.8.).

5.5.3. LN-18 cells, but not LN-229 cells, react differently to EGFR-specific (AG1478) versus bispecific EGFR/ErbB2-receptor inhibition (AEE788)

LN-18 cells (EGFR+++/ErbB2+) and LN-229 cells (EGFR+/ErbB2+++) were subjected to specific EGFR-inhibition with 5 µM AG1478 or bispecific EGFR/ErbB2-receptor inhibition with 5 µM AEE788 and the assay terminated 48 hours later by staining with crystal violet as described above (chapter 4.2.2. and 4.2.6.). The dose of 5 µM was selected as it was shown to exert marked growth inhibition on both cell lines using AEE788 (chapter 5.5.2., Fig. 5.8.).

LN-18 and LN-229 cells reacted differently to EGFR versus EGFR/ErbB2-receptor inhibition. LN-18 cells responded only weakly to sole EGFR-inhibition with 5 µM AG1478, but growth inhibition was marked after additional ErbB2-inhibition with AEE788 (Fig. 5.9.). There was a clear difference between treatment response to AG1478 versus AEE788 in LN-18 cells ($p < 0.001$) (Fig. 5.9.). In LN-229 cells no difference was detectable between growth-inhibition with AG1478 versus AEE788 (Fig. 5.9.).
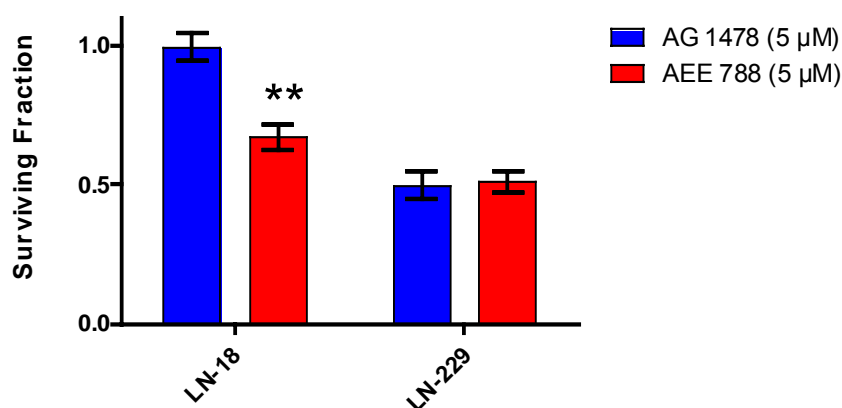
Figure 5.9. Efficacy of specific EGFR-inhibition (AG1478) versus bispecific EGFR/ErbB2-receptor inhibition (AEE788) on survival of LN-18 and LN-229 cells. Cells were incubated with 5μM AG1478 or AEE788 for 48 hours, stained with crystal violet, the absorbance measured at 570 nm and the surviving fraction calculated as percentage of control cell growth (0μM AG1478/AEE788). Error bars represent standard deviation of at least 24 replicate values. Asterixes indicate the significance of the growth-inhibiting difference between AG1478 versus AEE788 treatment as determined with two-way ANOVA and Bonferroni post-hoc test (** $p < 0.001$).

5.6. Evaluation of the major signalling pathways downstream to ErbB-receptors

5.6.1. PI3-kinase inhibition (LY294002) and MEK inhibition (PD98059) act differently on cell survival of LN-18 and LN-229 GBM cells

To evaluate the effect of PI3-kinase inhibition and MEK inhibition, LN-18 and LN-229 cells were incubated with LY294002 or PD98059 and the surviving fraction evaluated as described above (chapter 5.5., chapter 4.2.2. and 4.2.6.).

LY294002 exerted a clear dose-dependent growth-inhibiting effect on both cell lines starting at 0.1 μM for LN-229 cells ($p < 0.01$ at 0.1 μM, $p < 0.001$ at 1, 5, 10, 25 μM) (Fig. 5.10. B) and 1 μM for LN-18 cells ($p < 0.001$) (Fig. 5.10. A).

PD98059 showed different effects in the respective cell lines. It reacted well in LN-229 cells, causing dose-dependent growth inhibition commencing at 0.1 μM ($p < 0.001$) (Fig. 5.10. D). Contrary, a dose of 25 μM PD98059 was necessary to inhibit growth of LN-18 cells ($p < 0.001$) (Fig. 5.10. C).

A low-dose gowth-stimulating effect on LN-18 cells was observed with 0.1 μM LY294002 ($p < 0.01$). It did not reach statistical significance in LN-18 cells treated with PD98059.
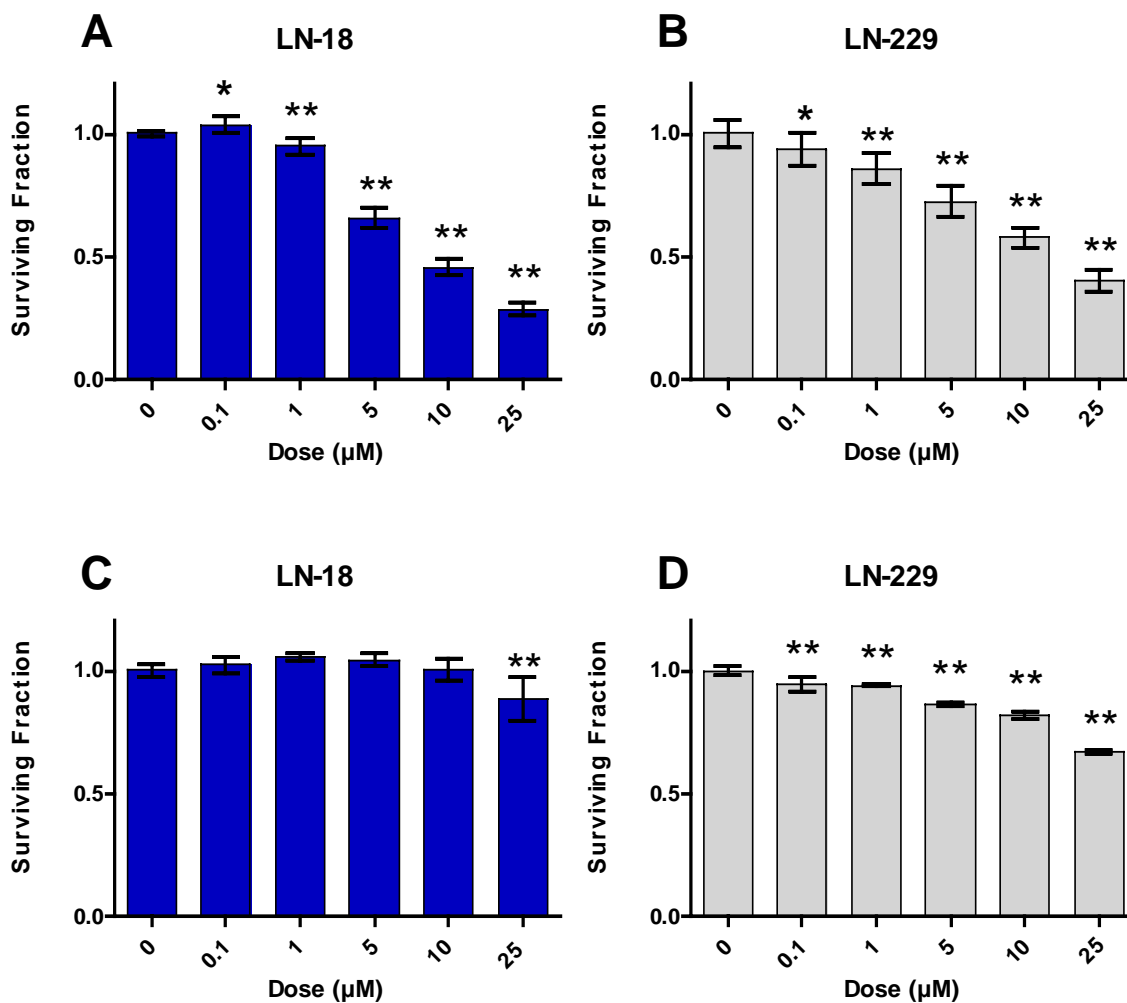
Figure 5.10. Effect of (A, B) PI3-kinase-Inhibitor LY294002 and (C, D) MEK-inhibitor PD98059 on LN-18 and LN-229 GBM cell lines. Cells were incubated with the indicated doses of inhibitor for 48 hours, stained with crystal violet, the absorbance measured at 570 nm and the surviving fraction calculated as percentage of control cell growth (0μM LY294002/PD98059). Error bars represent the standard deviation of at least 8 replicate values. Asterixes indicate the significance of the difference to control as determined using one-way ANOVA with Bonferroni post-hoc test (* $p < 0.01$; ** $p < 0.001$).

A

LY 294002 (µM)	-	-	**25**	-	-	-	-	-	-
AEE 788 (µM)	-	-	-	**5**	**10**	**25**	-	-	-
AG1478 (µM)	-	-	-	-	-	-	**5**	**10**	**25**
EGF (10ng/ml)	-	+	+	+	+	+	+	+	+

p-Akt ◄ 40 kDa

Akt ◄ 40 kDa

pp-44/42 MAPK ◄ 44/42 kDa

p-44/42 MAPK ◄ 44/42 kDa

1 2 3 4 5 6 7 8 9

B

LY 294002 (µM)	-	-	**25**	-	-	-	-	-	-
AEE 788 (µM)	-	-	-	**5**	**10**	**25**	-	-	-
AG1478 (µM)	-	-	-	-	-	-	**5**	**10**	**25**
EGF (10ng/ml)	-	+	+	+	+	+	+	+	+

p-Akt ◄ 40 kDa

Akt ◄ 40 kDa

pp-44/42 MAPK ◄ 44/42 kDa

p-44/42 MAPK ◄ 44/42 kDa

1 2 3 4 5 6 7 8 9
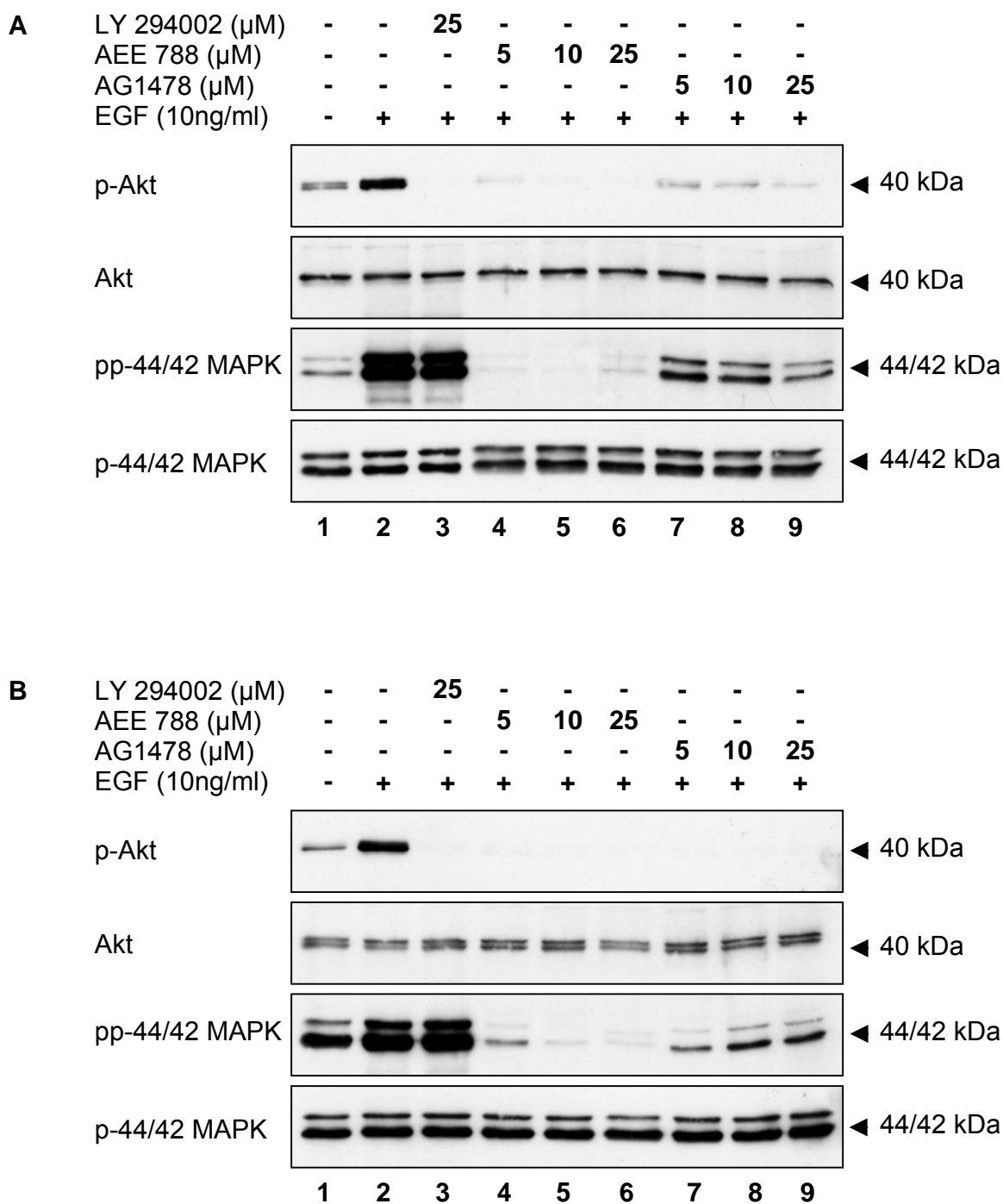
Figure 5.11. Effects of EGFR inhibition and bispecific EGFR/ErbB2-receptor inhibition on Akt and MAPK signalling pathways. (A) LN-18 and (B) LN-229 cells were treated with LY294002 (25 µM), AEE788 (5, 10, 25 µM) or AG1478 (5, 10, 25 µM) and epidermal growth factor (EGF, 10 ng/ml) as indicated, and the protein extracts analyzed by immunoblotting. To ensure equivalent loading and transfer, blots were probed concomitantly for p-Akt/ p-MAPK or pp-MAPK/Akt.

5.6.2. EGFR-specific (AG1478) and bispecific EGFR/ErbB2-receptor inhibition (AEE788) act differently on Akt and p-44/42 MAPK phosphorylation

For evaluation of downstream signalling pathway affection of EGFR-specific and bispecific EGFR/ErbB2-receptor inhibition, cells were incubated with 5, 10 or 25 μM AG1478 or AEE788 and 10 ng/ml EGF, followed by protein extraction and immunoblotting as described above (chapter 4.2.2. and 4.2.4.). 25 μM LY294002 served as control for the inhibition of the Akt/PI3K-pathway. To ensure equivalent loading and transfer, but avoid residual background noise from primary protein residues, blots were probed concomitantly for p-Akt/ p-MAPK or pp-MAPK/Akt.

Treatment had no impact on protein expression of non-activated Akt and p-44/42 MAPK. There was no decline in total Akt and MAPK expression in these experiments (Fig. 5.11. second and fourth panel in A and B). Both LN-18 and LN-229 cells showed a slight phosphorylation of Akt and p-44/42 MAPK in the absense of EGF, indicating a slight constitutive activation of both pathways (Fig. 5.11. line 1, first and third panel in A and B), albeit phosphorylation could be appreciably increased through addition of EGF (Fig. 5.11. line 2).

P-44/42 MAPK phosphorylation was more effectively blocked by AEE788 than by AG1478 in both cell lines (Fig. 5.11.).

LY294002 blocked Akt-phoshorylation in both cell lines, and had no effect on pp-44/42 MAPK. But it should be marked that blockage of Akt-phosphorylation by TKIs varied among LN-18 and LN-229 cells (Fig. 5.11. first panel in A and B), which was additionally visualized by optical density ratios in Fig. 5.12.

In LN-229 cells phosphorylation of p-Akt was equally strongly impeded by both AG1478 and AEE788, and no dose dependent effect could be disclosed (Fig. 5.11. B, first panel; Fig. 5.12.).

Contrary, and most interestingly, in LN-18 cells phosphorylation of p-Akt could be blocked more efficiently with AEE788 than with AG1478, and showed a clear dose-dependent effect (Fig. 5.11. A, first panel; Fig. 5.12.)
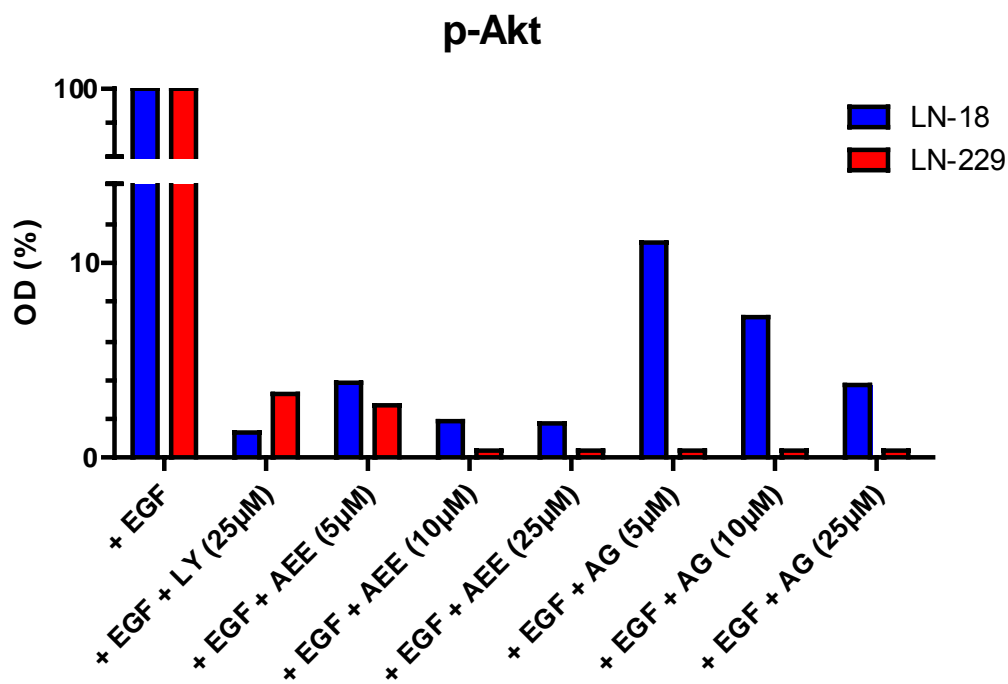
Figure 5.12. Optical density (OD) ratios of p-Akt levels of LN-18 and LN-229 cells pictured in Figure 5.11. Optical density was measured using ImageJ software 1.37v. Ordinate units represent percent to the activated non-inhibited control. LY: LY294002; AEE: AEE788; AG: AG1478.
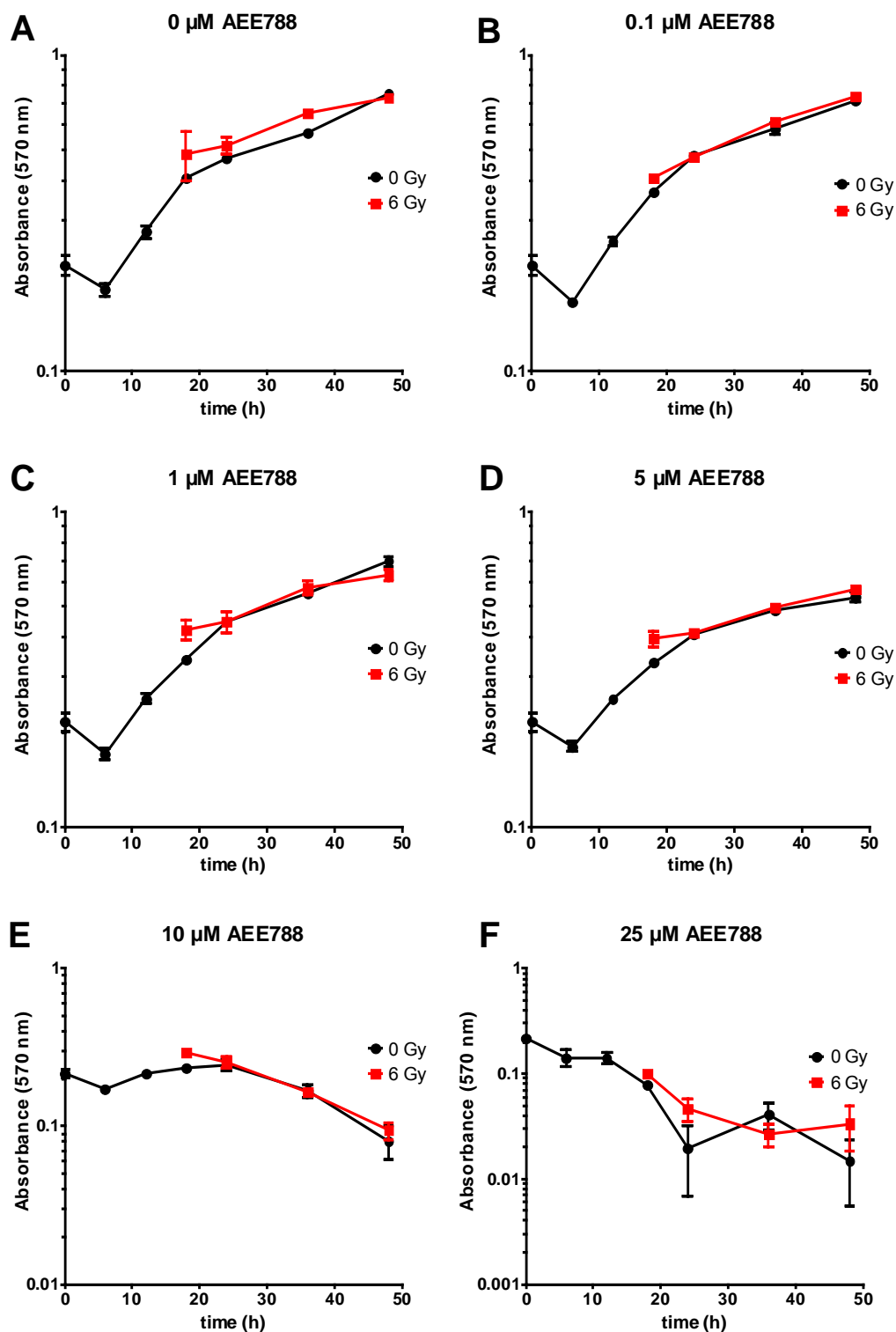
Figure 5.13. Effect of increasing concentrations of AEE788 with or without concomitant irradiation (6 Gy) on LN-18 glioma cells. Cells were treated with the indicated doses of AEE788, irradiated and growth inhibition evaluated 6, 12, 18, 24, 36 and 48 hours after AEE788-treatment. Data points represent the mean of direct measurement values. Error bars depict the standard deviation of at least eight replicate values.
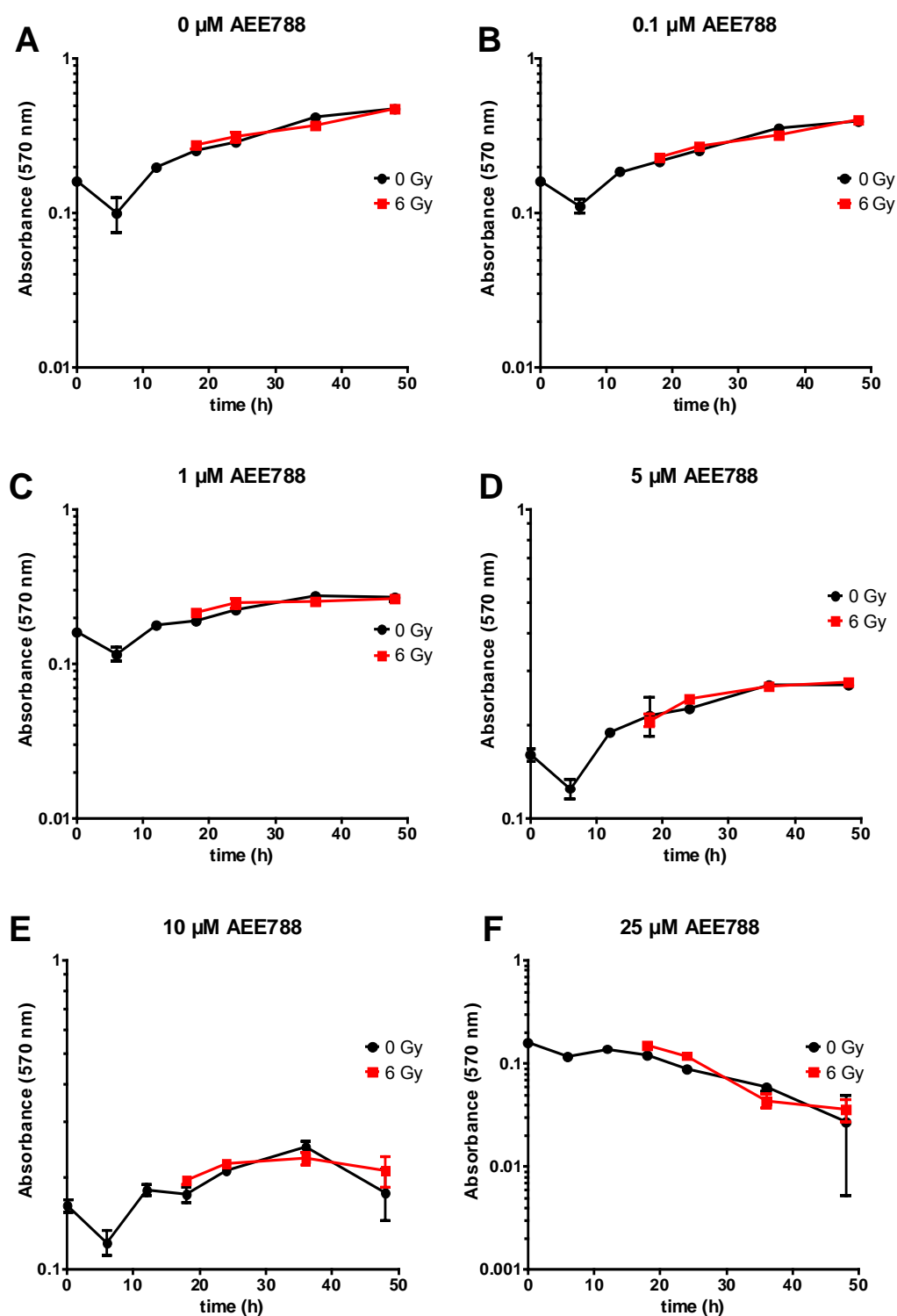
Figure 5.14. Effect of increasing concentrations of AEE788 with or without concomitant irradiation (6 Gy) on LN-229 glioma cells. Cells were treated with the indicated doses of AEE788, irradiated and growth inhibition evaluated 6, 12, 18, 24, 36 and 48 hours after AEE788-treatment. Data points represent the mean of direct measurement values. Error bars depict the standard deviation of at least eight replicate values.

5.7. Evaluation of radiosensitizing properties of specific EGFR-inhibition (AG1478) and bispecific EGFR/ErbB2-inhibition (AEE788) in LN-18 and LN-229 glioma cells

5.7.1. The short term cytotoxicity assay does not disclose radiosensitization of glioma cells with AEE788.

LN-18 and LN-229 cells were treated with increasing doses of AEE788 with or without concomitant irradiation with 6Gy, and growth inhibition was evaluated 6, 12, 18, 24, 36 and 48 hours after AEE788-treatment as described above (chapter 4.2.2. and 4.2.6.).

In both cell lines cell number (being linear to absorbance at 570 nm; see chapter 5.4.) decreased during the first 6 hours after inhibitor-treatment, most probably due to acute stress imposed by change of medium. AEE788 exerted a dose dependent effect as described in chapter 5.5.2. But no difference could be discerned between treatment with AEE788 only or concomitant irradiation with 6 Gy (Fig. 5.13.; Fig. 5.14.). The short term cytotoxicity assay did not disclose a radiosensitizing effect of AEE788 neither on LN-18 nor on LN-229 glioma cells.

5.7.2. The Colony-formation-assay shows a radiosensitizing property of the bispecific EGFR/ErbB2-inhibitor AEE788 on LN-18 glioma cells.

To examine dose-response clonogenic survival, LN-18 and LN-229 cells were treated with 5 µM AEE788 or 5 µM AG1478 with or without combined γ-irradiation with single doses of 2, 4, 6, 8 or 10 Gy (chapter 4.2.2.). After 10 days the colony forming potential was evaluated as described above (chapter 4.2.7.). Preliminary experiments using 25 µM AEE788 revealed excessive cytotoxicity leaving no space for evaluation of radiation-induced effects (data not shown). Hence the dosage of inhibitors was chosen to be 5 µM as it caused a marked, yet not overshooting response on cell survival in both cell lines (chapter 5.5.2.). Detailed analysis of dose-response was conducted using the linear-quadratic model as described in chapter 4.2.8. Computed α and β values, D_{37} and dose-enhancement ratios for each survival curve (Fig. 5.16.) are presented in table 5.2.

Both cell lines showed dose-dependent growth-inhibiting effects induced by irradiation with and without TKIs (Fig. 5.15. and Fig. 1.16.). Fitting survival fractions of LN-18 control-cells into the linear-quadratic equation resulted in paradoxically negative α values. As α-values

determine the initial slope of the survival curve, this at first sight paradoxic result may indicate slight growth stimulation of LN-18 cells at low doses of irradiation. Addition of TKIs showed abrogation of this effect, AEE788 being more efficient than AG1478.
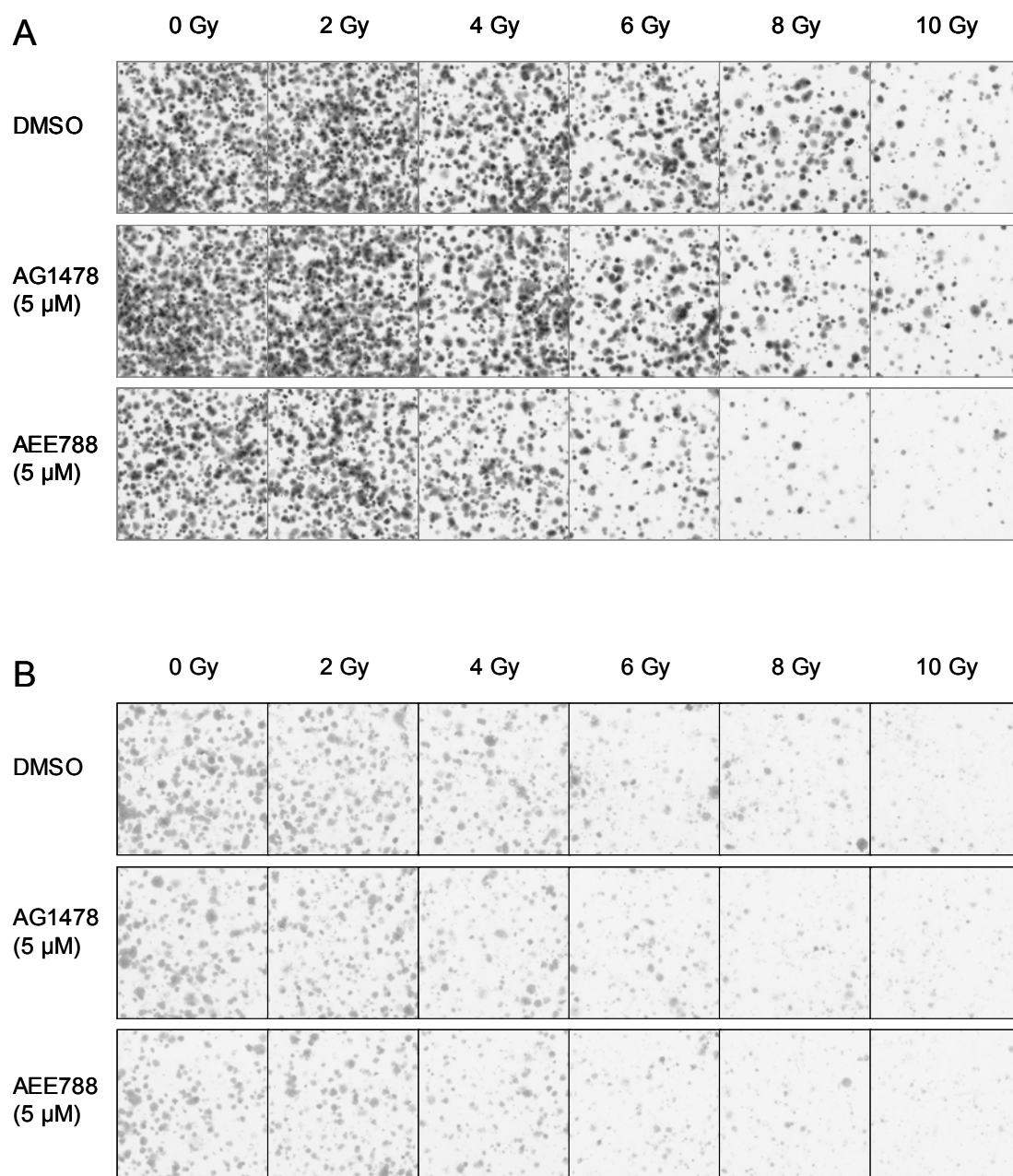
Figure 5.15. Dose-response clonogenic survival experiments. (A) LN-18 and (B) LN-229 cells were treated with 5 μM AEE788 or 5 μM AG1478 with or without concomitant γ-irradiation with single doses of 2, 4, 6, 8 or 10 Gy. DMSO treated cells served as controls.
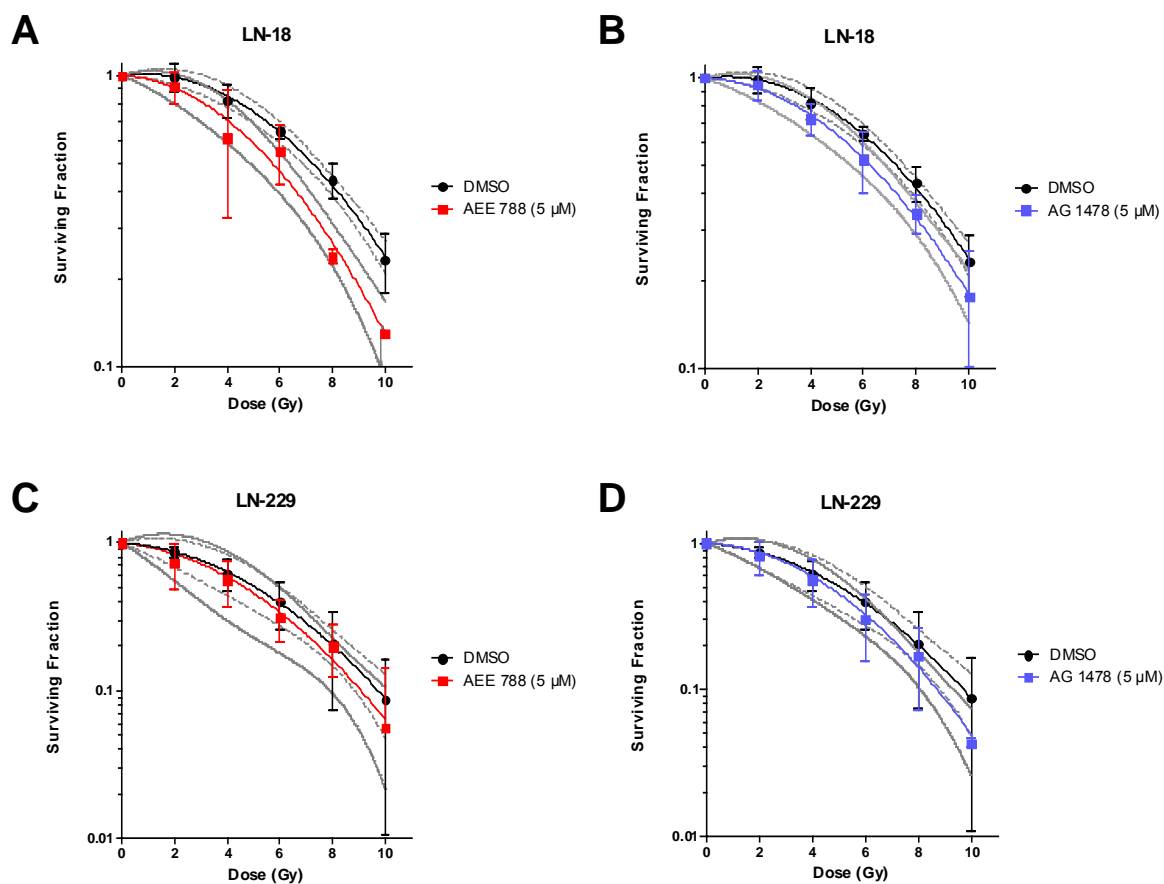
Figure 5.16. Dose-response clonogenic survival curves of (A, B) LN-18 and (C, D) LN-229 cells using the linear-quadratic model. Cells were treated with 5 µM AEE788 or 5 µM AG1478 with or without concomitant γ-irradiation with single doses of 2, 4, 6, 8 or 10 Gy. DMSO treated cells served as controls. Points represent the average of three independent experiments and error bars depict the standard deviation. Dotted lines represent the 95% confidence band of DMSO-survival curves and solid grey lines the 95% confidence band of AG1478/AEE788-survival curves. Graphs were generated using Prism software, version 5.0.

Cell line		DMSO	AG1478 (5µM)	AEE788 (5µM)
LN-18	α	-0.0282	0.0070	0.0097
	β	0.0171	0.0164	0.0194
	D_{37} (Gy)	8.49	7.58	6.91
	DER		1.12	1.23
LN-229	α	0.0273	0.0172	0.0383
	β	0.0216	0.0283	0.0237
	D_{37} (Gy)	6.18	5.63	5.72
	DER		1.10	1.08

Table 5.2. Linear-quadratic survival parameters of the survival curves presented in Figure 5.16. α and β are adjustable parameters in the linear-quadratic equation, $S = \exp(-\alpha D - \beta D^2)$, where S is the surviving fraction and D the radiation dose. D_{37} ist the radiation dose resulting in 37 % survival compared to non-irradiated controls. Dose-enhancement ratio (DER) was calculated as the quotient of D_{37} (radiation alone) and D_{37} (radiation plus inhibitor). Calculations were made using Prism software, version 5.0.

D_{37}, the radiation dose resulting in 37 % survival, was computed for each survival curve and the enhancement ratio for each inhibitor acquired by comparison of D_{37} of TKI-treated cells to controls.

D_{37} of AG1478-treated LN-18 cells and of both AG1478- and AEE788-treated LN-229 cells failed to show statistical difference to irradiated but TKI-untreated control cells (overlapping 95 % confidence bands) (Fig. 5.16.; B, C and D), although a trend towards enhanced growth-inhibition was discernable as the dose-enhancement ratio (DER) was greater than 1 (Table 5.2.).

Contrary, and most importantly though, in LN-18 cells treated with 5 µM AEE788 the dose enhancement ratio (DER) was 1.23 and the D_{37} differed to irradiated but TKI-untreated controls on the 5 % niveau (non-overlapping 95 % confidence bands) (Fig. 5.16.). This result indicates a radiosensitizing property of the bispecific EGFR/ErbB2-inhibitor AEE788 in LN-18 glioma cells.

6.   Discussion

Glioblastoma (GBM) is one of the most malignant human neoplasms and highly resistant to current standard therapies, consisting of cytoreductive surgery, radiation and chemotherapy. Novel therapeutic options are therefore especially necessary in the treatment of this invariably highly lethal disease.

During the last decade, EGFR has emerged as one of the most important targets for drug development in oncology, and seems especially promising in the treatment of GBM, which is highly dependent on epidermal growth factor receptor (EGFR) signalling (Ohgaki et al., 2004). Individualized EGFR-targeted therapy of GBM did not show the expected effects in clinical studies though (Chakravarti et al., 2006; Haas-Kogan et al., 2005; Rich et al., 2004; Van Den Bent et al., 2007).

Therefore, the aim of this study was to elucidate additional receptor dependency of growth-inhibiting and radiosensitizing effects of tyrosine kinase inhibitors (TKIs) targeting EGFR, and to evaluate the efficacy of additional concomitant ErbB2-receptor inhibition.

Growth-inhibiting effects of specific EGFR- and bispecific EGFR/ErbB2-TKIs in glioma cell lines with different EGFR/ErbB2 co-expression patterns disclosed the importance of ErbB2-receptor signalling. Most interestingly, an unexpected sensitivity of ErbB2-receptor overexpressing cells to specific EGFR-TKI was disclosed, and additional ErbB2-inhibition was shown to overcome the resistance of EGFR overexpressing cells to specific EGFR-TKI. Clonogenic experiments showed a radiosensitizing effect of bispecific EGFR/ErbB2-inhibitors in EGFR overexpressing glioma cells, further highlighting the importance of ErbB2-receptor inhibition in EGFR driven tumors. Finally, immunoblot analyses and evaluation of growth-inhibition induced by specific inhibitors of effector molecules downstream to EGFR/ErbB2 disclosed that the growth-inhibiting effects of EGFR and ErbB2 inhibition are most likely mediated through the PI3K/Akt signalling pathway.

6.1.   Evaluation of the experimental design

Evaluation of EGFR and ErbB2-receptor signalling in glioma cells was conducted using specific EGFR and bispecific EGFR/ErbB2-receptor inhibitors. The three inhibitors were well characterized with regard to their kinase-specificity both in enzyme studies and cell-based assays (chapter 4.1.4.). AG1478 was proven to selectively inhibit EGFR (Levitzki and Gazit, 1995). PKI166 and AEE788 were both designed as bispecific EGFR and ErbB2-receptor

inhibitors, among which AEE788 exerted greater potency at ErbB2-receptor inhibition (Traxler et al., 2004; Traxler et al., 2001). AEE788 being a new compound, its ability to inhibit EGFR/ErbB2 signalling in glioma cells was to be validated (chapter 5.1.).

Selective inhibition of ErbB2-receptor could not be applied, as no selective ErbB2-inhibitors were available. Some authors claim tyrphostin AG825 to be a suitable compound. But AG825 achieves selective ErbB2 inhibition only in an ATP-depleted environment and consequently is known to loose selectivity for ErbB2 in intact-cell assays (Osherov et al., 1993).

Evaluation of the two major signalling pathways downstream to EGFR/ErbB2-receptor was conducted by means of two well-characterized inhibitors with proven selectivity both in enzyme studies and cell-based assays. LY294002 was shown to target the Akt cascade by selective inhibition of the PI3-kinase (Vlahos et al., 1994). PD98059 is known to affect the MAPK cascade by specific inhibition of MAPK kinase (MEK) (Dudley et al., 1995; Pang et al., 1995; Vlahos et al., 1994) (chapter 4.1.4.).

The cell lines LN-18 (EGFR+++/ErbB2+) and LN-229 (EGFR+/ErbB2+++) were chosen as a model for the investigation of EGFR and ErbB2 targeted therapy in GBM. They presented an inverse ratio of EGFR and ErbB2 respectively, as determined by FACS analysis and immunoblotting (chapter 5.2. and 5.3.). Furthermore, both originated from *de novo* GBM, a subgroup known to rely on ErbB signalling (chapter 2.3.2.). For assessment of any contribution of ErbB induced Akt signalling it was of high importance that both cell lines presented a wild type PTEN-status (Ishii et al., 1999). LN-229 showed no constitutive activation of Akt, and the apparent constitutive activation of the Akt signalling pathway in LN-18 cells reported before was most likely due to a strong overexpression of EGFR, as it could be overcome upon treatment with the EGFR-inhibitor AG1478 (Schlegel et al., 2000). Additionally, both cell lines expressed p53 protein (Kraus et al., 1999), which was important in order to exclude radiosensitizing effects due to lack of p53 function (Haas-Kogan et al., 1999). All genetic characteristics listed above identified LN-18 and LN-229 cells as the most suitable model for the investigation of EGFR and ErbB2 targeted therapy in GBM.

The effects on cell proliferation exerted by treatment with inhibitors and γ-irradiation were evaluated by two different well-established methods.
(a) Short term growth-inhibition up to 48 hours after treatment was assessed using the crystal violet staining assay based on the method of Gillies (Gillies et al., 1986) and Saotome

(Saotome et al., 1989), where cellular nucleoproteins are stained by crystal violet followed by cell lysis and subsequent measurement of absorbance of the solubilized dye (chapter 4.2.6.). Relative cell number is then deducted from the colorimetric difference to control. A crucial precondition is the correspondence of absorbance to viable cell number, which was shown for various cell lines before (HeLa cells, Chinese hamster lung cells, mouse fibroblasts), but is known to go missing when culture is continued after reaching confluence (Chiba et al., 1998; Gillies et al., 1986; Itagaki et al., 1991; Saotome et al., 1989).

To confirm reliability of the assay for LN-18 and LN-229 glioma cells, a clear linear relationship between cell number and absorbance was demonstrated within the range of cell numbers tested (chapter 5.4.). Furthermore, a well-chosen inoculum size assured that cells were assayed before reaching confluence – avoiding this major pitfall of the crystal violet staining method.

In summary, the crystal violet staining assay is a well-established and reproducible growth-inhibition assay designed for cell quantification only, regardless of biological activity (Yung, 1989).

(b) For evaluation of radiation-induced growth-effects and radiosensitization, the proliferative potential of cells was focused on by assessing their colony formation ability based on the method introduced by Puck (Puck and Marcus, 1956) (chapter 4.2.7). It is crucial to remember, that cells lethally damaged by irradiation do not immediately cease activity, but may continue multiplying for as much as 5 generations before terminating their reproduction. Accurate count of true colony-forming survivors 10 days after treatment was therefore achieved by the standard method of counting only colonies consisting of at least 50 cells (Puck and Marcus, 1956). Automated counting of colonies by image analysis was based on the method of Dahle et al. (Dahle et al., 2004), and was specifically designed to identify merging colonies, enabling proper colony count even in case of densely populated dishes. The surviving fractions determined by the difference of colony numbers of treated cells to controls were fitted into the classical linear-quadratic equation, widely accepted as the most accurate model for single-dose radiation induced cell response (Contessa et al., 2006; Hall, 1994).

Immunoblot analyses were conducted using a protocol standard to our laboratory. Equal protein quantities as determined with the Bradford protein quantification assay were loaded onto each line. To ensure equivalent loading and transfer, blots were probed concomitantly for p-Akt/p-MAPK and pp-MAPK/Akt, or a tubulin control was conducted.

6.2. Discussion of the results

6.2.1. The bispecific EGFR/ErbB2-receptor tyrosine kinase inhibitor AEE788 shows a strong inhibiting effect on EGFR/ErbB2-heterodimer signalling in glioma cell lines

Assessing the effect of AEE788 on EGFR and ErbB2 signalling in glioma cells, the present study suggests a pronounced EGFR/ErbB2-heterodimer formation following EGF-stimulation with and without additional inhibition by AEE788. Even though no substances faciliating co-immunoprecipitation were added, strong ErbB2-receptor protein bands were observed after immunoprecipitation of EGFR (Fig. 5.1.). This is consistent with ErbB2 being widely accepted as the preferred dimerization partner for all ErbB receptors (Yarden and Sliwkowski, 2001). It furthermore affirms previous result showing EGF-induced prefered formation of EGFR/ErbB2-heterodimers (versus EGFR-homodimers) in other malignant neoplasms, e.g. in human squamous cell carcinoma cells (Gulliford et al., 1997).

Stimulation by EGF produced marked receptor phosphorylation and downregulation of total EGFR and ErbB2-receptor, known to take place following receptor stimulation (Yarden and Sliwkowski, 2001).

The present study shows that clinically relevant doses of 1 µM AEE788 (Failly et al., 2007) cause complete inhibition of EGF-induced EGFR and ErbB2-receptor activation in LN-18 cells, and furthermore impair receptor downregulation as indicated by strong protein bands of total EGFR and ErbB2-receptor (Fig. 5.1.). Similar results were shown for LN-229 cells (Failly et al., 2007).

6.2.2. Efficiency of EGFR targeted therapy depends on the relative cellular amount of EGFR to ErbB2-receptors

Exploration of EGFR/ErbB2 inhibition using the model of two glioblastoma cell lines with an inverse ratio of EGFR and ErbB2-receptor revealed an unexpected relative resistance of presumably EGFR-driven LN-18 cells (EGFR+++/ErbB2+) to sole EGFR inhibition with AG1478 at low concentrations (chapter 5.5., Fig. 5.5.). Most interestingly though, the resistance could be overcome by additionally targeting ErbB2-receptor with the bispecific EGFR/ErbB2-receptor inhibitors PKI166 and AEE788 (chapter 5.5., Fig.5.6.). And even among this bispecific compounds efficacy to inhibit cell-growth seemed to correlate directly

with the intinsic potency to block the ErbB2-receptor, hence AEE788 was superior over PKI166.

Contrary, ErbB2-overexpressing LN-229 cells (EGFR+/ErbB2+++) reacted equally well to low concentration EGFR inhibiton, regardless of additional ErbB2-receptor inhibition (chapter 5.5.).

For further elucidation, cellular responses to equimolar doses of 5 µM inhibitor were compared. It seemed most appropriate to choose the dosage of 5 µM AEE788, as it proved to exert marked growth inhibition, yet avoiding the overshooting cytotoxic effects of higher dosages, being possibly assigned to a loss of specificity for EGFR and ErbB2-receptor inhibition (chapter 5.5.2., Fig. 5.8.).

This approach clearly confirmed the different behaviour of LN-18 and LN-229 cells faced with EGFR or concomitant EGFR/ErbB2-inhibition. LN-18 cells (EGFR+++/ErbB2+) showed no response to sole EGFR inhibition with 5µM AG1478, but significant growth-inhibition followed additional ErbB2-receptor inhibition with 5 µM AEE788. LN-229 cells (EGFR+/ErbB2+++) reacted equally well to both compounds, showing a uniform decrease of the surviving fraction by about 50% (chapter 5.5.3., Fig. 5.9.).

In conclusion, the experimental data lead to the hypothesis that responsiveness to EGFR targeted therapy might depend on the relative quantity of EGFR compared to ErbB2-receptor instead of EGFR overexpression only, as currently believed. Indeed, the present study indicates that overexpression of EGFR in tumor cells expressing comparably less ErbB2-receptor may not only fail to serve as a positive predictive marker for response to EGFR targeted therapy, but even render cells resistant to it.

This may explain why in various tumors EGFR expression has not proven to be a useful predictive marker to EGFR-targeted therapies neither in preclinical studies, where EGFR-inhibition resulted in growth arrest of tumors expressing a wide range of EGFR levels (Sirotnak et al., 2000; Wakeling et al., 2002), nor in clinical settings (Campiglio et al., 2004; Johnson and Arteaga, 2003). In cell based and xenograft experiments using the specific EGFR TKIs AG1478 or gefitinib, ErbB2-overexpression was suggested to indicate responsiveness to EGFR targeted therapy (Emlet et al., 2006; Moasser et al., 2001; Moulder et al., 2001). The data presented here are consistent with this observation, though it shall be additionally claimed that rather than total receptor amount, the relation of EGFR to ErbB2-receptors may be crucial for response to EGFR targeted therapy.

A conclusive hypothetical explanation may be the impaired EGFR/ErbB2-heterodimer formation induced by bispecific EGFR/ErbB2-inhibition in LN-18 cells and both EGFR-specific and bispecific EGFR/ErbB2-inhibition in LN-229 cells (Fig. 6.1.). Signalling through ErbB2-heterodimers is widely accepted to be superior in strength and duration over ErbB-homodimer signalling (Yarden and Sliwkowski, 2001), and EGFR/ErbB2-heterodimers are preferentially formed following EGF-stimulation (Gulliford et al., 1997). The enhanced signalling potency and preferred formation identify EGFR/ErbB2-heterodimers as main effectors of the oncogenic potential of ErbB receptors, and thus pivotal for the proliferation of ErbB dependent cancer cells.

Transferring this knowledge into a mechanistic explanation of the present findings, EGFR-inhibition in EGFR-overexpressing LN-18 cells (EGFR+++/ErbB2+) does not interfere with EGFR/ErbB2-heterodimer signalling, and hence induces no growth inhibiting effect. Thereby it is implied that due to EGFR-overexpression the total amount of EGFR is only partially blocked by the specific EGFR TKI AG1468. Concomitant inhibition of the comparably lower amount of ErbB2-receptor – implying a complete receptor blockage due to the low receptor number – impairs heterodimer formation inducing marked growth inhibition (Fig. 6.1.).
In LN-229 cells (EGFR+/ErbB2+++) harbouring comparably less EGFR while overexpressing ErbB2-receptor, sole EGFR inhibition is sufficient to inhibit EGFR/ErbB2-heterodimer formation – a complete blockage of EGFR is implied by both EGFR and EGFR/ErbB2 TKIs (Fig. 6.1.).

In support of this hypothetical model and of the importance of heterodimer signalling, recent clinical observations disclosed an adverse prognostic value of ErbB2-overexpression in breast cancer patients only when ErbB2 was in the activated (i.e. phosphorylated) state or co-expressed with EGFR (DiGiovanna et al., 2005). Thereby 97 % of tumors expressing activated ErbB2 co-expressed EGFR (DiGiovanna et al., 2005), highlighting the importance and prognostic value of ligand-dependent, i.e. ErbB-dimerization-partner dependent mechanisms of ErbB2 activation. In another clinical observation in patients with non-small-cell lung cancer, sensitivity of EGFR-positive tumors treated with the specific EGFR-inhibitor gefitinib was associated with increased copy numbers of the ErbB2 gene (Cappuzzo et al., 2005).

Additional support for the hypothetical model presented (Fig. 6.1.) would be highly desirable though. It must be acknowledged, that a subtotal inhibition of EGFR-activation (i.e. phosphorylation) by 5 µM AG1478 in LN-18 cells is suggested, which remains to be validated. Furthermore, additional backing for the hypothesis could result from evaluating homo- and hetero-receptorinteractions resulting from concomitant specific EGFR- or bispecific EGFR/ErbB2-inhibition using the flow cytometric Fluorescence Resonance Energy Transfer (FRET) technique. Cell lines stably overexpressing graded levels of EGFR and ErbB2 would be another conceivable experimental approach for further verification of the hypothesis presented above.
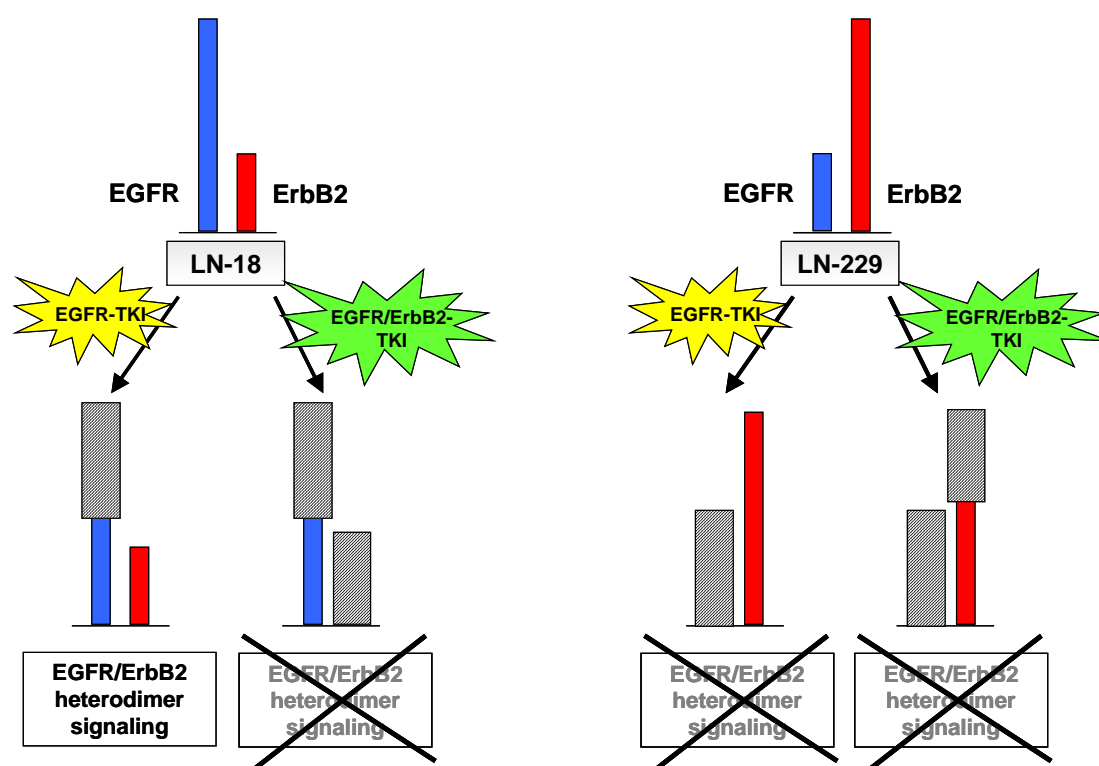
Figure 6.1. Hypothetical mechanistic model for the effect of specific EGFR- and bispecific EGFR/ErbB2-inhibition on EGFR/ErbB2-heterodimer formation in cells with an inverse ratio of EGFR and ErbB2-receptor. Blue bars represent the relative cellular amount of EGFR; red bars represent the relative cellular amount of ErbB2-receptor. Striped bars indicate inhibition of receptors.

6.2.3. Response to inhibition of EGFR and ErbB2-receptor with TKIs is mainly mediated through the Akt signalling pathway

Downstream effects of EGFR and EGFR/ErbB2 signalling are known to be mediated, in a large measure, by the MAPK and the PI3-K/Akt-pathways (Yarden and Sliwkowski, 2001). Hence it was of interest to investigate the effect of specific EGFR inhibition (using AG1478) and bispecific EGFR/ErbB2-receptor inhibition (using AEE788) on the activation of Akt and MAPK.

For both LN-18 and LN-229 cells immunoblot analyses revealed a comparable reduction of phosphorylated (i.e. activated) MAPK after addition of inhibitors, of which bispecific EGFR/ErbB2 inhibition proved more potent than specific EGFR inhibition in both cell lines equally (Fig. 5.11.). This appears to suggest that relative resistance of LN-18 cells to the effects of sole EGFR inhibition exerted by AG1478 is not mediated through MAPK signalling.

Phosphorylation (i.e. activation) of Akt was blocked uniformly by both EGFR- and EGFR/ErbB2-inhibition in LN-229 cells, even at low inhibitor dosages. Contrary, in LN-18 cells Akt phosphorylation (i.e. activation) was blocked far more efficiently by bispecific EGFR/ErbB2 inhibition than by EGFR-inhibition only, and showed a clear dose dependency (Fig. 5.12.).

Evaluating growth-inhibiting effects induced by specific inhibition of the PI3-K/Akt-pathway by LY294002 versus specific inhibition of the MAPK-pathway by PD98059, LN-18 showed a relative resistance for the MEK-inhibitor PD98059 (Fig. 5.10. C), both cell lines reacting equally well to PI3K-inhibition by LY294002 (Fig. 5.10. A and B).

Inhibition of the PI3K/Akt-pathway was thereby shown to correlate with the growth suppressing effects of EGFR and EGFR/ErbB2-receptor inhibition (Fig. 5.5.), suggesting that the PI3K/Akt-pathway may be important in driving tumor growth in both EGFR- and ErbB2-overexpressing GBM. Consistently, activation of the PI3K/Akt-pathway has been found to be associated with reduced survival of glioma patients and it is significantly more frequent in GBM than in non-GBM astrocytic tumors (Chakravarti et al., 2004b).

Furthermore and most importantly, it is hypothesized that the relative resistance of LN-18 cells to sole EGFR-inhibition may be mediated through an incomplete blockage of Akt-signalling, which can be overcome by additional inhibition of the ErbB2-receptor. This claim

is consistent with a recent clinical study disclosing Akt phosphorylation as the strongest predictor of lack of response to EGFR-targeted therapy in GBM (Haas-Kogan et al., 2005).

6.2.4. The bispecific EGFR/ErbB2-receptor inhibitor AEE788 radiosensitizes LN-18 but not LN-229 GBM cells

ErbB receptors are known to be activated by ionizing radiation to produce radioprotective cellular responses accounting for at least part of the radioresistance of cancer cells (Contessa et al., 2002; Nyati et al., 2006). This leads to the assumption that inhibition of ErbB receptors with TKIs may prove a valuable radiosensitizing approach. Matching expectations, EGFR-inhibitors have up to date proven to exert some radiosensitizing properties in preclinical and clinical settings in various solid tumors, even though controversial results were also reported (Baumann et al., 2007; Riesterer et al., 2007). In GBM cell based studies it was even shown that inhibition of the Akt signalling pathways with the PI3K-Inhibitor LY294002 mediates radiosensitisation (Nakamura et al., 2005).

Unfortunately though, LY294002 is not suitable for clinical use owing to its small therapeutic window (Riesterer et al., 2004), and EGFR targeted therapy and irradiation in GBM patients showed up to date only disappointing clinical results (Chakravarti et al., 2006). This may have several reasons, most importantly being presumably kinase dependence and proper patient selection (Arteaga and Baselga, 2004), leading to the need to augment preclinical understanding of underlying principles of ErbB-inhibition mediated radiosensitization. One aim of the present study was therefore to evaluate the benefit of specific EGFR versus bispecific EGFR/ErbB2 inhibition following radiotherapy of glioma cells.

Detailed analysis was conducted using the standard linear-quadratic model (chapter 4.2.8.). As α determines the initial slope of the curve, the at first sight paradoxic result of negative α-values for the untreated but irradiated LN-18 cells may well represent growth stimulation at low doses of radiation, consistent with former results reporting activation of the ErbB receptors by low dose radiation (Schmidt-Ullrich et al., 2003).

In irradiated LN-229 cells (EGFR+/ErbB2+++) only a trend towards increased growth inhibition after treatment with both EGFR- or EGFR/ErbB2-receptor-inhibitors was discernable, which did not reach statistical significance (C and D in Fig. 5.16.).

In the EGFR-overexpressing LN-18 cells (EGFR+++/ErbB2+) though, the unexpected observation was made, that EGFR/ErbB2-inhibition resulted in radiosensitization starting at a dose of 6 Gy (A in Fig. 5.16.), whereas sole EGFR inhibition was not sufficient to significantly enhance radiosensitivity (B in Fig. 5.16.). This conclusion is driven from a significantly lower radiation dose needed to reduce cell survival to 37 % in EGFR/ErbB2-inhibitor pretreated cells versus untreated controls (D_{37} in Table 5.2.).

6.3.   Clinical relevance

Of course, it cannot be assumed that results obtained on cell lines *in vitro* can be translated directly into the clinic. Even though, the findings presented here may have significant clinical relevance.

Prospective selection or exclusion of patients into clinical trials based on molecular characteristics is becoming a reality, and the disappointing results obtained with EGFR TKIs to date are most probably due to so far undisclosed molecular characteristics of the neoplasms (Arteaga and Baselga, 2004). Therefore, preclinical studies arise as a *sine qua non* for successful clinical applications, providing insight on molecular characteristics rendering patients susceptive to individualized targeted therapy.

Consequentially, policies of drug-approving institutions like the FDA strongly encourage development of predictive markers for molecular targeted therapeutic compounds. This great need for predictive markers in Oncology renders the present study highly valuable.

The data presented here suggest, that although EGFR TKIs are developed as "targeted therapies" selective for EGFR overexpressing tumors, their clinical testing should not be confined to patients with EGFR-overexpressing neoplasms. Moreover, it shall be claimed that clinical efficacy could well be dependent from ErbB2-overexpression, or from the relative expression of EGFR and ErbB2-receptors.

It shall be furthermore suggested, that resistance of EGFR-overexpressing GBM to EGFR-targeted therapies may be overcome through additional concomitant inhibition of the ErbB2-receptor with bispecific EGFR/ErbB2 TKIs.

The clinical significance of the present results concerning radiosensitizing properties of the bispecific EGFR/ErbB2-receptor inhibitor AEE788 in LN-18 cells may be of great impact.

It was shown that AEE788 has the propensity to radiosensitize glioma cells overexpressing EGFR and co-expressing ErbB2. And although the dose enhancement ratio was only moderate *in vitro* (DER = 1.23), it may well translate to substantial synergy *in vivo*, as reported in similar settings before (Nyati et al., 2004).

This may have several reasons. First of all, considering fractionated administration of radiation, the moderate DER of 1.23 per fraction (reported in this study) for each of e.g. 15 fractions would result in a substantial total enhancement ratio of 22.3 (1.23^{15}). Additionally, effects on *in vivo* tumor microenvironment like angiogenesis may further promote *in vivo* efficacy. ErbB TKI have been described to block the secretion of angiogenic factors such as vascular endothelial growth factor (VEGF) and interleukin-8 (De Luca et al., 2008), and AEE788 is known to exert direct antiangiogenic activity through additional VEGF-inhibition (Traxler et al., 2004).

6.4.   Conclusion

GBM may show co-expression of EGFR and ErbB2-receptor and the data of the present study lead to four major observations:

First, they confirm the importance of ErbB2-receptor signalling in ErbB-targeted therapy of GBM. In both cell lines regardless of the relative cellular amounts of EGFR and ErbB2-receptor, growth-inhibiting efficacy of the TKIs increased with the their propensity to inhibit the ErbB2-receptor, the effect being most likely due to impairment of EGFR/ErbB2 heterodimer signalling.

Second, rather than EGFR amount, ErbB2-overexpression may indicate responsiveness to EGFR targeted therapy. In the present study EGFR-overexpressing cells were resistant to specific EGFR-inhibition, whereas ErbB2-overexpressing cells – harbouring only comparably less EGFR – showed an unexpected sensitivity to specific EGFR-inhibition, which could not be significantly enhanced by additional ErbB-inhibition.

Third, and most interestingly, it was shown that resistance of EGFR-overexpressing glioma cells to EGFR-targeted therapy may be overcome by additional concomitant ErbB2-receptor inhibition using bispecific EGFR/ErbB2-TKIs. Furthermore, the results suggest that this

effect – and the response to inhibition of EGFR and ErbB2-receptor in general – is mainly mediated through the PI3K/Akt signalling pathway.

As the fourth and last point, a radiosensitizing effect of bispecific EGFR/ErbB2-inhibitors in EGFR-overexpressing glioma cells was revealed, further highlighting the importance of ErbB2-receptor inhibition in EGFR driven tumors.

Taken together the results of the present study disclose the importance of ErbB2-receptor signalling in EGFR targeted therapy of glioblastoma. Additionally it shall be claimed that rather than total individual receptor amount, it may well be the cellular ratio of EGFR to ErbB2-receptor which determines response to EGFR targeted therapy.

7.   Summary/Abstract

Glioblastoma (GBM) is among the most malignant of all human neoplasms, with dismal patient outcome. It is one of the most treatment-refractory tumors and shows high levels of resistance to conventional therapies (i.e. surgery, irradiation, and chemotherapy). This bleak patient prognosis presents urgent necessity for new therapeutic options.

One highly promissing approach is the rational development of new therapies targeting molecules in cancer specific signalling pathways, thereby ideally increasing efficacy and minimizing toxicity. Targeted inhibition of the ErbB class of growth factor receptors including the epidermal growth factor receptor (EGFR) seems especially promising in GBM, as it is known that overexpression of EGFR presents a key signalling pathway in *de novo* GBM. ErbB receptor signalling is induced by ligand dependent homo- or heterodimerization of individual receptor-monomers (ErbB1 – 4), which triggers signal transduction mainly through the PI3K/Akt- and MAPK-pathways. Thereby it is most notable that ErbB2 acts as a "non-autonomous amplifier": it fails to form homodimers, but serves as the prefered dimerization partner for other ErbB receptors with signalling potency of ErbB2-heterodimers markedly exceeding those of homodimers.

One method to inhibit ErbB receptors is the administration of specific small-molecule tyrosine kinase inhibitors (TKIs), cell-permeable agents that inhibit the protein tyrosine kinase activity, which is responsible for downstream signalling of the receptors.

EGFR targeting TKIs proved effective in other solid cancers, but showed only dissappointing effects in GBM. This may have several reasons, most important being presumably kinase dependence and proper patient selection.

The aim of the present study was therefore to elucidate additional receptor dependency of growth-inhibiting and radiosensitizing effects of EGFR-specific TKIs and assess the efficacy of additional ErbB2-receptor inhibition by bispecific EGFR/ErbB2 TKIs.

After assessing the EGFR and ErbB2-receptor status by FACS-analysis and immunoblotting, two cell lines with an inverse ratio of EGFR and ErbB2-receptor were selected as the most appropriate experimental model: LN-18 (EGFR+++/ErbB2+) and LN-229 (EGFR+/ErbB2+). Treatment with either specific EGFR TKI (AG1478) or bispecific EGFR/ErbB2-TKIs (PKI166 and AEE788) disclosed the importance of ErbB2-receptor signalling in glioma cell lines. In both cell lines bispecific EGFR/ErbB2 TKIs showed a higher growth-inhibiting efficacy than specific EGFR TKI – the growth inhibiting effect being proportional to the

propensity of the TKIs to inhibit the ErbB2-receptor, and therefore most likely due to impairment of EGFR/ErbB2 heterodimer signalling. Importantly, the EGFR-overexpressing cells LN-18 (EGFR+++/ErbB2+) were resistant to specific EGFR inhibition, and ErbB2-overexpressing cells LN-229 (EGFR+/ErbB2+++) showed an unexpected sensitivity to specific EGFR inhibition. Most interestingly, the resistance of EGFR-overexpressing cells to EGFR-targeted therapy could be overcome by additional concomitant ErbB2-receptor inhibition using bispecific EGFR/ErbB2-TKIs.

Evaluation of radiation-induced growth-effects conducting clonogenic experiments disclosed a significant radiosensitizing effect of the bispecific EGFR/ErbB2-inhibitor AEE788 in EGFR-overexpressing LN-18 cells (EGFR+++/ErbB2+), thereby further highlighting the importance of ErbB2-inhibition in EGFR driven tumors.

Finally, the PI3K/Akt- and the MAPK-pathway were focused on, representing the major signalling pathways downstream to EGFR and ErbB2-receptor. Immunoblot analyses following specific EGFR and bispecific EGFR/ErbB2 inhibition and evaluation of growth-inhibition induced by specific inhibitors of the PI3K/Akt and MAPK pathways suggested, that the growth-inhibiting effects of EGFR and EGFR/ErbB2 TKIs are most likely mediated through the PI3K/Akt signalling pathway. This is especially true for the additional concomitant ErbB2-inhibition overcoming resistance of EGFR-overexpressing cells to EGFR inhibition.

Taken together, the results of the present study disclose the importance of ErbB2-receptor signalling in EGFR targeted therapy of Glioblastoma. The data suggest, that rather than EGFR amount, ErbB2 overexpression may indicate responsiveness to EGFR targeted therapy, including radiosensitizing properties. Furthermore, it was shown that resistance to EGFR targeted therapy may be overcome by additional inhibition of the ErbB2-receptor. Thus it shall be claimed, that responsiveness to EGFR targeted therapy may rather depend from the relation of EGFR to ErbB2-receptors than from total individual receptor amount.

8. References

Arteaga, C.L., and J. Baselga. 2004. Tyrosine kinase inhibitors: why does the current process of clinical development not apply to them? *Cancer Cell*. 5:525-31.

Baselga, J., F. Rojo, H. Dumez, A. Mita, C.H. Takimoto, J. Tabernero, C. Dilea, K. Parker, M. Dugan, and A.T. van Oosterom. 2005. Phase I study of AEE788, a novel multitargeted inhibitor of ErbB and VEGF receptor family tyrosine kinases: A pharmacokinetic (PK) - pharmacodynamic (PD) study to identify the optimal therapeutic dose regimen. *J Clin Oncol*. 23, ASCO Annual Meeting Proceedings:S3028.

Baulida, J., M.H. Kraus, M. Alimandi, P.P. Di Fiore, and G. Carpenter. 1996. All ErbB receptors other than the epidermal growth factor receptor are endocytosis impaired. *J Biol Chem*. 271:5251-7.

Baumann, M., M. Krause, E. Dikomey, K. Dittmann, W. Dorr, U. Kasten-Pisula, and H.P. Rodemann. 2007. EGFR-targeted anti-cancer drugs in radiotherapy: preclinical evaluation of mechanisms. *Radiother Oncol*. 83:238-48.

Biernat, W., P. Kleihues, Y. Yonekawa, and H. Ohgaki. 1997. Amplification and overexpression of MDM2 in primary (de novo) glioblastomas. *J Neuropathol Exp Neurol*. 56:180-5.

Bradford, M.M. 1976. A rapid and sensitive method for the quantitation of microgram quantities of protein utilizing the principle of protein-dye binding. *Anal Biochem*. 72:248-54.

Brockhoff, G., P. Heiss, J. Schlegel, F. Hofstaedter, and R. Knuechel. 2001. Epidermal growth factor receptor, c-erbB2 and c-erbB3 receptor interaction, and related cell cycle kinetics of SK-BR-3 and BT474 breast carcinoma cells. *Cytometry*. 44:338-48.

Brognard, J., A.S. Clark, Y. Ni, and P.A. Dennis. 2001. Akt/protein kinase B is constitutively active in non-small cell lung cancer cells and promotes cellular survival and resistance to chemotherapy and radiation. *Cancer Res*. 61:3986-97.

Campiglio, M., A. Locatelli, C. Olgiati, N. Normanno, G. Somenzi, L. Vigano, M. Fumagalli, S. Menard, and L. Gianni. 2004. Inhibition of proliferation and induction of apoptosis in breast cancer cells by the epidermal growth factor receptor (EGFR) tyrosine kinase inhibitor ZD1839 ('Iressa') is independent of EGFR expression level. *J Cell Physiol*. 198:259-68.

Cappuzzo, F., M. Varella-Garcia, H. Shigematsu, I. Domenichini, S. Bartolini, G.L. Ceresoli, E. Rossi, V. Ludovini, V. Gregorc, L. Toschi, W.A. Franklin, L. Crino, A.F. Gazdar, P.A. Bunn, Jr., and F.R. Hirsch. 2005. Increased HER2 gene copy number is associated with response to gefitinib therapy in epidermal growth factor receptor-positive non-small-cell lung cancer patients. *J Clin Oncol*. 23:5007-18.

Carter, S., K.L. Auer, D.B. Reardon, M. Birrer, P.B. Fisher, K. Valerie, R. Schmidt-Ullrich, R. Mikkelsen, and P. Dent. 1998. Inhibition of the mitogen activated protein (MAP) kinase cascade potentiates cell killing by low dose ionizing radiation in A431 human squamous carcinoma cells. *Oncogene*. 16:2787-96.

Chakravarti, A., B. Berkey, H.I. Robins, A. Guha, W. Curran, D. Brachman, C. Shultz, and M. Mehta. 2006. An Update of Phase II Results From RTOG 0211: A Phase I/II Study of Gefitinib+Radiation for Newly-Diagnosed Glioblastoma Patients. *Int J Radiat Oncol Biol Phys*. 66:S83-84.

Chakravarti, A., M.A. Delaney, E. Noll, P.M. Black, J.S. Loeffler, A. Muzikansky, and N.J. Dyson. 2001. Prognostic and pathologic significance of quantitative protein expression profiling in human gliomas. *Clin Cancer Res*. 7:2387-95.

Chakravarti, A., A. Dicker, and M. Mehta. 2004a. The contribution of epidermal growth factor receptor (EGFR) signaling pathway to radioresistance in human gliomas: a review of preclinical and correlative clinical data. *Int J Radiat Oncol Biol Phys*. 58:927-31.

Chakravarti, A., G. Zhai, Y. Suzuki, S. Sarkesh, P.M. Black, A. Muzikansky, and J.S. Loeffler. 2004b. The prognostic significance of phosphatidylinositol 3-kinase pathway activation in human gliomas. *J Clin Oncol*. 22:1926-33.

Chiba, K., K. Kawakami, and K. Tohyama. 1998. Simultaneous Evaluation of Cell Viability by Neutral Red, MTT and Crystal Violet Staining Assays of the Same Cells. *Toxicology in Vitro*:251-258.

Citri, A., and Y. Yarden. 2006. EGF-ERBB signalling: towards the systems level. *Nat Rev Mol Cell Biol*. 7:505-16.

Cloughesy, T., A. Yung, J. Vrendenberg, K. Aldape, D. Eberhard, M. Prados, S. Vandenberg, B. Klencke, and P. Mischel. 2005. Phase II study of erlotinib in recurrent GBM: Molecular predictors of outcome. *J Clin Oncol*. 23, ASCO Annual Meeting Proceedings:S1507.

Contessa, J.N., A. Abell, K. Valerie, P.S. Lin, and R.K. Schmidt-Ullrich. 2006. ErbB receptor tyrosine kinase network inhibition radiosensitizes carcinoma cells. *Int J Radiat Oncol Biol Phys*. 65:851-8.

Contessa, J.N., J. Hampton, G. Lammering, R.B. Mikkelsen, P. Dent, K. Valerie, and R.K. Schmidt-Ullrich. 2002. Ionizing radiation activates Erb-B receptor dependent Akt and p70 S6 kinase signaling in carcinoma cells. *Oncogene*. 21:4032-41.

Dahle, J., M. Kakar, H.B. Steen, and O. Kaalhus. 2004. Automated counting of mammalian cell colonies by means of a flat bed scanner and image processing. *Cytometry A*. 60:182-8.

Davis, B.J. 1964. Disc Electrophoresis. Ii. Method and Application to Human Serum Proteins. *Ann N Y Acad Sci*. 121:404-27.

Dawson, J.P., M.B. Berger, C.C. Lin, J. Schlessinger, M.A. Lemmon, and K.M. Ferguson. 2005. Epidermal growth factor receptor dimerization and activation require ligand-induced conformational changes in the dimer interface. *Mol Cell Biol*. 25:7734-42.

De Luca, A., A. Carotenuto, A. Rachiglio, M. Gallo, M.R. Maiello, D. Aldinucci, A. Pinto, and N. Normanno. 2008. The role of the EGFR signaling in tumor microenvironment. *J Cell Physiol*. 214:559-67.

DiGiovanna, M.P., D.F. Stern, S.M. Edgerton, S.G. Whalen, D. Moore, 2nd, and A.D. Thor. 2005. Relationship of epidermal growth factor receptor expression to ErbB-2 signaling activity and prognosis in breast cancer patients. *J Clin Oncol*. 23:1152-60.

Diserens, A.C., N. de Tribolet, A. Martin-Achard, A.C. Gaide, J.F. Schnegg, and S. Carrel. 1981. Characterization of an established human malignant glioma cell line: LN-18. *Acta Neuropathol (Berl)*. 53:21-8.

Dropcho, E.J., and S.J. Soong. 1996. The prognostic impact of prior low grade histology in patients with anaplastic gliomas: a case-control study. *Neurology*. 47:684-90.

Dudley, D.T., L. Pang, S.J. Decker, A.J. Bridges, and A.R. Saltiel. 1995. A synthetic inhibitor of the mitogen-activated protein kinase cascade. *Proc Natl Acad Sci U S A*. 92:7686-9.

Emlet, D.R., R. Schwartz, K.A. Brown, A.A. Pollice, C.A. Smith, and S.E. Shackney. 2006. HER2 expression as a potential marker for response to therapy targeted to the EGFR. *Br J Cancer*. 94:1144-53.

Ermoian, R.P., C.S. Furniss, K.R. Lamborn, D. Basila, M.S. Berger, A.R. Gottschalk, M.K. Nicholas, D. Stokoe, and D.A. Haas-Kogan. 2002. Dysregulation of PTEN and protein kinase B is associated with glioma histology and patient survival. *Clin Cancer Res*. 8:1100-6.

Failly, M., S. Korur, V. Egler, J.L. Boulay, M.M. Lino, R. Imber, and A. Merlo. 2007. Combination of sublethal concentrations of epidermal growth factor receptor inhibitor and microtubule stabilizer induces apoptosis of glioblastoma cells. *Mol Cancer Ther*. 6:773-81.

Ferguson, K.M., M.B. Berger, J.M. Mendrola, H.S. Cho, D.J. Leahy, and M.A. Lemmon. 2003. EGF activates its receptor by removing interactions that autoinhibit ectodomain dimerization. *Mol Cell*. 11:507-17.

Fulci, G., M. Labuhn, D. Maier, Y. Lachat, O. Hausmann, M.E. Hegi, R.C. Janzer, A. Merlo, and E.G. Van Meir. 2000. p53 gene mutation and ink4a-arf deletion appear to be two mutually exclusive events in human glioblastoma. *Oncogene*. 19:3816-22.

Garrett, T.P., N.M. McKern, M. Lou, T.C. Elleman, T.E. Adams, G.O. Lovrecz, M. Kofler, R.N. Jorissen, E.C. Nice, A.W. Burgess, and C.W. Ward. 2003. The crystal structure of a truncated ErbB2 ectodomain reveals an active conformation, poised to interact with other ErbB receptors. *Mol Cell*. 11:495-505.

Gillies, R.J., N. Didier, and M. Denton. 1986. Determination of cell number in monolayer cultures. *Anal Biochem*. 159:109-13.

Goldberg, R.M. 2005. Cetuximab. *Nat Rev Drug Discov*. Suppl:S10-1.

Grossman, S.A., and J.F. Batara. 2004. Current management of glioblastoma multiforme. *Semin Oncol*. 31:635-44.

Gulliford, T.J., G.C. Huang, X. Ouyang, and R.J. Epstein. 1997. Reduced ability of transforming growth factor-alpha to induce EGF receptor heterodimerization and downregulation suggests a mechanism of oncogenic synergy with ErbB2. *Oncogene*. 15:2219-23.

Haas-Kogan, D.A., S.S. Kogan, G. Yount, J. Hsu, M. Haas, D.F. Deen, and M.A. Israel. 1999. p53 function influences the effect of fractionated radiotherapy on glioblastoma tumors. *Int J Radiat Oncol Biol Phys*. 43:399-403.

Haas-Kogan, D.A., M.D. Prados, T. Tihan, D.A. Eberhard, N. Jelluma, N.D. Arvold, R. Baumber, K.R. Lamborn, A. Kapadia, M. Malec, M.S. Berger, and D. Stokoe. 2005. Epidermal growth factor receptor, protein kinase B/Akt, and glioma response to erlotinib. *J Natl Cancer Inst*. 97:880-7.

Hall, E.J. 1994. Cell Survival Curves. *In* Radiobiology for the Radiologist. J.B. Lippincott Company, Philadelphia.

Hanahan, D., and R.A. Weinberg. 2000. The hallmarks of cancer. *Cell*. 100:57-70.

Hegi, M.E., A.C. Diserens, T. Gorlia, M.F. Hamou, N. de Tribolet, M. Weller, J.M. Kros, J.A. Hainfellner, W. Mason, L. Mariani, J.E. Bromberg, P. Hau, R.O. Mirimanoff, J.G. Cairncross, R.C. Janzer, and R. Stupp. 2005. MGMT gene silencing and benefit from temozolomide in glioblastoma. *N Engl J Med*. 352:997-1003.

Holbro, T., and N.E. Hynes. 2004. ErbB receptors: directing key signaling networks throughout life. *Annu Rev Pharmacol Toxicol*. 44:195-217.

Ishii, N., D. Maier, A. Merlo, M. Tada, Y. Sawamura, A.C. Diserens, and E.G. Van Meir. 1999. Frequent co-alterations of TP53, p16/CDKN2A, p14ARF, PTEN tumor suppressor genes in human glioma cell lines. *Brain Pathol*. 9:469-79.

Itagaki, H., S. Hagino, S. Kato, T. Kobayashi, and M. Umeda. 1991. An *in vitro* alternative to the Draize eye-irritation test: evaluation of the crystal violet staining method. *Toxicology in Vitro*:139-143.

Johnson, D.H., and C.L. Arteaga. 2003. Gefitinib in recurrent non-small-cell lung cancer: an IDEAL trial? *J Clin Oncol*. 21:2227-9.

Jordan, C.T., M.L. Guzman, and M. Noble. 2006. Cancer stem cells. *N Engl J Med*. 355:1253-61.

Kantarjian, H., C. Sawyers, A. Hochhaus, F. Guilhot, C. Schiffer, C. Gambacorti-Passerini, D. Niederwieser, D. Resta, R. Capdeville, U. Zoellner, M. Talpaz, B. Druker, J. Goldman, S.G. O'Brien, N. Russell, T. Fischer, O. Ottmann, P. Cony-Makhoul, T. Facon, R. Stone, C. Miller, M. Tallman, R. Brown, M. Schuster, T. Loughran, A. Gratwohl, F. Mandelli, G. Saglio, M. Lazzarino, D. Russo, M. Baccarani, and E. Morra. 2002. Hematologic and cytogenetic responses to imatinib mesylate in chronic myelogenous leukemia. *N Engl J Med*. 346:645-52.

Kapoor, G.S., and D.M. O'Rourke. 2003. Receptor tyrosine kinase signaling in gliomagenesis: pathobiology and therapeutic approaches. *Cancer Biol Ther*. 2:330-42.

Keime-Guibert, F., O. Chinot, L. Taillandier, S. Cartalat-Carel, M. Frenay, G. Kantor, J.S. Guillamo, E. Jadaud, P. Colin, P.Y. Bondiau, P. Menei, H. Loiseau, V. Bernier, J. Honnorat, M. Barrie, K. Mokhtari, J.J. Mazeron, A. Bissery, and J.Y. Delattre. 2007. Radiotherapy for glioblastoma in the elderly. *N Engl J Med*. 356:1527-35.

Kim, H.H., U. Vijapurkar, N.J. Hellyer, D. Bravo, and J.G. Koland. 1998. Signal transduction by epidermal growth factor and heregulin via the kinase-deficient ErbB3 protein. *Biochem J*. 334 (Pt 1):189-95.

Klapper, L.N., S. Glathe, N. Vaisman, N.E. Hynes, G.C. Andrews, M. Sela, and Y. Yarden. 1999. The ErbB-2/HER2 oncoprotein of human carcinomas may function solely as a

shared coreceptor for multiple stroma-derived growth factors. *Proc Natl Acad Sci U S A*. 96:4995-5000.

Kleihues, P., P.C. Burger, and B.W. Scheithauer. 1993. Histological typing of tumors of the central nervous system. *In* World Health Organization Classification of Tumors of the Central Nervous System. Springer Verlag., Berlin.

Kraus, A., M.W. Gross, R. Knuechel, K. Munkel, F. Neff, and J. Schlegel. 2000. Aberrant p21 regulation in radioresistant primary glioblastoma multiforme cells bearing wild-type p53. *J Neurosurg*. 93:863-72.

Kraus, A., F. Neff, M. Behn, M. Schuermann, K. Muenkel, and J. Schlegel. 1999. Expression of alternatively spliced mdm2 transcripts correlates with stabilized wild-type p53 protein in human glioblastoma cells. *Int J Cancer*. 80:930-4.

Krause, D.S., and R.A. Van Etten. 2005. Tyrosine kinases as targets for cancer therapy. *N Engl J Med*. 353:172-87.

Lacroix, M., D. Abi-Said, D.R. Fourney, Z.L. Gokaslan, W. Shi, F. DeMonte, F.F. Lang, I.E. McCutcheon, S.J. Hassenbusch, E. Holland, K. Hess, C. Michael, D. Miller, and R. Sawaya. 2001. A multivariate analysis of 416 patients with glioblastoma multiforme: prognosis, extent of resection, and survival. *J Neurosurg*. 95:190-8.

Laemmli, U.K. 1970. Cleavage of structural proteins during the assembly of the head of bacteriophage T4. *Nature*. 227:680-5.

Langlois, W.J., T. Sasaoka, A.R. Saltiel, and J.M. Olefsky. 1995. Negative feedback regulation and desensitization of insulin- and epidermal growth factor-stimulated p21ras activation. *J Biol Chem*. 270:25320-3.

Lenferink, A.E., R. Pinkas-Kramarski, M.L. van de Poll, M.J. van Vugt, L.N. Klapper, E. Tzahar, H. Waterman, M. Sela, E.J. van Zoelen, and Y. Yarden. 1998. Differential endocytic routing of homo- and hetero-dimeric ErbB tyrosine kinases confers signaling superiority to receptor heterodimers. *Embo J*. 17:3385-97.

Levitzki, A., and A. Gazit. 1995. Tyrosine kinase inhibition: an approach to drug development. *Science*. 267:1782-8.

Louis, D.N., H. Ohgaki, O.D. Wiestler, and W.K. Cavenee. 2007. World Health Organization Classification of Tumors of the Central Nervous System. IARC, Lyon.

Lynch, T.J., D.W. Bell, R. Sordella, S. Gurubhagavatula, R.A. Okimoto, B.W. Brannigan, P.L. Harris, S.M. Haserlat, J.G. Supko, F.G. Haluska, D.N. Louis, D.C. Christiani, J. Settleman, and D.A. Haber. 2004. Activating mutations in the epidermal growth factor

receptor underlying responsiveness of non-small-cell lung cancer to gefitinib. *N Engl J Med*. 350:2129-39.

Mayer-Proschel, M., A.J. Kalyani, T. Mujtaba, and M.S. Rao. 1997. Isolation of lineage-restricted neuronal precursors from multipotent neuroepithelial stem cells. *Neuron*. 19:773-85.

Mellinghoff, I.K., M.Y. Wang, I. Vivanco, D.A. Haas-Kogan, S. Zhu, E.Q. Dia, K.V. Lu, K. Yoshimoto, J.H. Huang, D.J. Chute, B.L. Riggs, S. Horvath, L.M. Liau, W.K. Cavenee, P.N. Rao, R. Beroukhim, T.C. Peck, J.C. Lee, W.R. Sellers, D. Stokoe, M. Prados, T.F. Cloughesy, C.L. Sawyers, and P.S. Mischel. 2005. Molecular determinants of the response of glioblastomas to EGFR kinase inhibitors. *N Engl J Med*. 353:2012-24.

Mineo, J.F., A. Bordron, M. Baroncini, C.A. Maurage, C. Ramirez, R.M. Siminski, C. Berthou, and P. Dam Hieu. 2007. Low HER2-expressing glioblastomas are more often secondary to anaplastic transformation of low-grade glioma. *J Neurooncol*. 85:281-7.

Mischel, P.S., and T.F. Cloughesy. 2003. Targeted molecular therapy of GBM. *Brain Pathol*. 13:52-61.

Moasser, M.M., A. Basso, S.D. Averbuch, and N. Rosen. 2001. The tyrosine kinase inhibitor ZD1839 ("Iressa") inhibits HER2-driven signaling and suppresses the growth of HER2-overexpressing tumor cells. *Cancer Res*. 61:7184-8.

Moulder, S.L., F.M. Yakes, S.K. Muthuswamy, R. Bianco, J.F. Simpson, and C.L. Arteaga. 2001. Epidermal growth factor receptor (HER1) tyrosine kinase inhibitor ZD1839 (Iressa) inhibits HER2/neu (erbB2)-overexpressing breast cancer cells in vitro and in vivo. *Cancer Res*. 61:8887-95.

Nakamura, J.L., A. Karlsson, N.D. Arvold, A.R. Gottschalk, R.O. Pieper, D. Stokoe, and D.A. Haas-Kogan. 2005. PKB/Akt mediates radiosensitization by the signaling inhibitor LY294002 in human malignant gliomas. *J Neurooncol*. 71:215-22.

Nakamura, M., T. Watanabe, U. Klangby, C. Asker, K. Wiman, Y. Yonekawa, P. Kleihues, and H. Ohgaki. 2001. p14ARF deletion and methylation in genetic pathways to glioblastomas. *Brain Pathol*. 11:159-68.

Nyati, M.K., D. Maheshwari, S. Hanasoge, A. Sreekumar, S.D. Rynkiewicz, A.M. Chinnaiyan, W.R. Leopold, S.P. Ethier, and T.S. Lawrence. 2004. Radiosensitization by pan ErbB inhibitor CI-1033 in vitro and in vivo. *Clin Cancer Res*. 10:691-700.

Nyati, M.K., M.A. Morgan, F.Y. Feng, and T.S. Lawrence. 2006. Integration of EGFR inhibitors with radiochemotherapy. *Nat Rev Cancer*. 6:876-85.

Ohgaki, H., P. Dessen, B. Jourde, S. Horstmann, T. Nishikawa, P.L. Di Patre, C. Burkhard, D. Schuler, N.M. Probst-Hensch, P.C. Maiorka, N. Baeza, P. Pisani, Y. Yonekawa, M.G. Yasargil, U.M. Lutolf, and P. Kleihues. 2004. Genetic pathways to glioblastoma: a population-based study. *Cancer Res*. 64:6892-9.

Ohgaki, H., and P. Kleihues. 2005. Epidemiology and etiology of gliomas. *Acta Neuropathol*. 109:93-108.

Ohgaki, H., and P. Kleihues. 2007. Genetic pathways to primary and secondary glioblastoma. *Am J Pathol*. 170:1445-53.

Olayioye, M.A., R.M. Neve, H.A. Lane, and N.E. Hynes. 2000. The ErbB signaling network: receptor heterodimerization in development and cancer. *Embo J*. 19:3159-67.

Ornstein, L. 1964. Disc Electrophoresis. I. Background and Theory. *Ann N Y Acad Sci*. 121:321-49.

Osherov, N., A. Gazit, C. Gilon, and A. Levitzki. 1993. Selective inhibition of the epidermal growth factor and HER2/neu receptors by tyrphostins. *J Biol Chem*. 268:11134-42.

Paez, J.G., P.A. Janne, J.C. Lee, S. Tracy, H. Greulich, S. Gabriel, P. Herman, F.J. Kaye, N. Lindeman, T.J. Boggon, K. Naoki, H. Sasaki, Y. Fujii, M.J. Eck, W.R. Sellers, B.E. Johnson, and M. Meyerson. 2004. EGFR mutations in lung cancer: correlation with clinical response to gefitinib therapy. *Science*. 304:1497-500.

Pang, L., T. Sawada, S.J. Decker, and A.R. Saltiel. 1995. Inhibition of MAP kinase kinase blocks the differentiation of PC-12 cells induced by nerve growth factor. *J Biol Chem*. 270:13585-8.

Panikkar, R.P., I. Astsaturov, and C.J. Langer. 2008. The emerging role of cetuximab in head and neck cancer: a 2007 perspective. *Cancer Invest*. 26:96-103.

Peiffer, J., and P. Kleihues. 1999. Hans-Joachim Scherer (1906-1945), pioneer in glioma research. *Brain Pathol*. 9:241-5.

Puck, T.T., and P.I. Marcus. 1956. Action of x-rays on mammalian cells. *J Exp Med*. 103:653-66.

Raizer, J.J., L.E. Abrey, P. Wen, T. Cloughesy, I.A. Robins, H.A. Fine, F. Lieberman, V.K. Puduvalli, K.L. Fink, and M. Prados. 2004. A phase II trial of erlotinib (OSI-774) in patients (pts) with recurrent malignant gliomas (MG) not on EIAEDs. *J Clin Oncol*. 22, ASCO Annual Meeting Proceedings:S1502.

Reardon, D.A., T. Cloughesy, C. Conrad, M. Prados, J. Xia, W. Mietlowski, M. Dugan, P. Mischel, H. Friedman, and A. Yung. 2005. A phase I study of AEE788, a novel

multitarget inhibitor of ErbB and VEGF receptor family tyrosine kinases, in recurrent GBM patients. *J Clin Oncol*. 23, ASCO Annual Meeting Proceedings:S3063.

Rich, J.N., and D.D. Bigner. 2004. Development of novel targeted therapies in the treatment of malignant glioma. *Nat Rev Drug Discov*. 3:430-46.

Rich, J.N., D.A. Reardon, T. Peery, J.M. Dowell, J.A. Quinn, K.L. Penne, C.J. Wikstrand, L.B. Van Duyn, J.E. Dancey, R.E. McLendon, J.C. Kao, T.T. Stenzel, B.K. Ahmed Rasheed, S.E. Tourt-Uhlig, J.E. Herndon, 2nd, J.J. Vredenburgh, J.H. Sampson, A.H. Friedman, D.D. Bigner, and H.S. Friedman. 2004. Phase II trial of gefitinib in recurrent glioblastoma. *J Clin Oncol*. 22:133-42.

Riesterer, O., L. Milas, and K.K. Ang. 2007. Use of molecular biomarkers for predicting the response to radiotherapy with or without chemotherapy. *J Clin Oncol*. 25:4075-83.

Riesterer, O., A. Tenzer, D. Zingg, B. Hofstetter, V. Vuong, M. Pruschy, and S. Bodis. 2004. Novel radiosensitizers for locally advanced epithelial tumors: inhibition of the PI3K/Akt survival pathway in tumor cells and in tumor-associated endothelial cells as a novel treatment strategy? *Int J Radiat Oncol Biol Phys*. 58:361-8.

Rubin, I., and Y. Yarden. 2001. The basic biology of HER2. *Ann Oncol*. 12 Suppl 1:S3-8.

Saotome, K., H. Morita, and M. Umeda. 1989. Cytotoxicity test with simplified crystal violet staining method using microtitre plates and its application to injection drugs. *Toxic. in Vitro*. 3:317-321.

Scherer, H. 1940. Cerebral astrocytomas and their derivatives. *Am j Cancer*. 40:159-98.

Schlegel, J., G. Piontek, B. Budde, F. Neff, and A. Kraus. 2000. The Akt/protein kinase B-dependent anti-apoptotic pathway and the mitogen-activated protein kinase cascade are alternatively activated in human glioblastoma multiforme. *Cancer Lett*. 158:103-8.

Schlegel, J., G. Stumm, K. Brandle, A. Merdes, G. Mechtersheimer, N.E. Hynes, and M. Kiessling. 1994. Amplification and differential expression of members of the erbB-gene family in human glioblastoma. *J Neurooncol*. 22:201-7.

Schmidt-Ullrich, R.K., J.N. Contessa, P. Dent, R.B. Mikkelsen, K. Valerie, D.B. Reardon, G. Bowers, and P.S. Lin. 1999. Molecular mechanisms of radiation-induced accelerated repopulation. *Radiat Oncol Investig*. 7:321-30.

Schmidt-Ullrich, R.K., J.N. Contessa, G. Lammering, G. Amorino, and P.S. Lin. 2003. ERBB receptor tyrosine kinases and cellular radiation responses. *Oncogene*. 22:5855-65.

Sirotnak, F.M., M.F. Zakowski, V.A. Miller, H.I. Scher, and M.G. Kris. 2000. Efficacy of cytotoxic agents against human tumor xenografts is markedly enhanced by

coadministration of ZD1839 (Iressa), an inhibitor of EGFR tyrosine kinase. *Clin Cancer Res*. 6:4885-92.

Stebbing, J., E. Copson, and S. O'Reilly. 2000. Herceptin (trastuzamab) in advanced breast cancer. *Cancer Treat Rev*. 26:287-90.

Stupp, R., W.P. Mason, M.J. van den Bent, M. Weller, B. Fisher, M.J. Taphoorn, K. Belanger, A.A. Brandes, C. Marosi, U. Bogdahn, J. Curschmann, R.C. Janzer, S.K. Ludwin, T. Gorlia, A. Allgeier, D. Lacombe, J.G. Cairncross, E. Eisenhauer, and R.O. Mirimanoff. 2005. Radiotherapy plus concomitant and adjuvant temozolomide for glioblastoma. *N Engl J Med*. 352:987-96.

Tomlinson, F.H., B.W. Scheithauer, C.J. Hayostek, J.E. Parisi, F.B. Meyer, E.G. Shaw, T.L. Weiland, J.A. Katzmann, and C.R. Jack, Jr. 1994. The significance of atypia and histologic malignancy in pilocytic astrocytoma of the cerebellum: a clinicopathologic and flow cytometric study. *J Child Neurol*. 9:301-10.

Traxler, P., P.R. Allegrini, R. Brandt, J. Brueggen, R. Cozens, D. Fabbro, K. Grosios, H.A. Lane, P. McSheehy, J. Mestan, T. Meyer, C. Tang, M. Wartmann, J. Wood, and G. Caravatti. 2004. AEE788: a dual family epidermal growth factor receptor/ErbB2 and vascular endothelial growth factor receptor tyrosine kinase inhibitor with antitumor and antiangiogenic activity. *Cancer Res*. 64:4931-41.

Traxler, P., G. Bold, E. Buchdunger, G. Caravatti, P. Furet, P. Manley, T. O'Reilly, J. Wood, and J. Zimmermann. 2001. Tyrosine kinase inhibitors: from rational design to clinical trials. *Med Res Rev*. 21:499-512.

Tzahar, E., and Y. Yarden. 1998. The ErbB-2/HER2 oncogenic receptor of adenocarcinomas: from orphanhood to multiple stromal ligands. *Biochim Biophys Acta*. 1377:M25-37.

Uhm, J.H., K.W. Ballman, C. Giannini, J.C. Krauss, J.C. Buckner, D. James, B.W. Scheithauer, J.R. O'Fallon, and K.A. Jaeckle. 2004. Phase II study of ZD1839 in patients with newly diagnosed grade 4 astrocytoma. *J Clin Oncol*. 22, ASCO Annual Meeting Proceedings:S1505.

Van Den Bent, M.J., A. Brandes, R. Rampling, M. Kouwenhoven, J.M. Kros, A.F. Carpentier, P. Clement, B. Klughammer, T. Gorlia, and D. Lacombe. 2007. Randomized phase II trial of erlotinib (E) versus temozolomide (TMZ) or BCNU in recurrent glioblastoma multiforme (GBM): EORTC 26034. *J Clin Oncol (Meeting Abstracts)*. 25:2005.

Vlahos, C.J., W.F. Matter, K.Y. Hui, and R.F. Brown. 1994. A specific inhibitor of phosphatidylinositol 3-kinase, 2-(4-morpholinyl)-8-phenyl-4H-1-benzopyran-4-one (LY294002). *J Biol Chem*. 269:5241-8.

Wakeling, A.E., S.P. Guy, J.R. Woodburn, S.E. Ashton, B.J. Curry, A.J. Barker, and K.H. Gibson. 2002. ZD1839 (Iressa): an orally active inhibitor of epidermal growth factor signaling with potential for cancer therapy. *Cancer Res*. 62:5749-54.

Watanabe, K., O. Tachibana, K. Sata, Y. Yonekawa, P. Kleihues, and H. Ohgaki. 1996. Overexpression of the EGF receptor and p53 mutations are mutually exclusive in the evolution of primary and secondary glioblastomas. *Brain Pathol*. 6:217-23; discussion 23-4.

Weinstein, I.B. 2002. Cancer. Addiction to oncogenes--the Achilles heal of cancer. *Science*. 297:63-4.

Weiss, A., and J. Schlessinger. 1998. Switching signals on or off by receptor dimerization. *Cell*. 94:277-80.

Wen, P.Y., W.K. Yung, K.R. Lamborn, P.L. Dahia, Y. Wang, B. Peng, L.E. Abrey, J. Raizer, T.F. Cloughesy, K. Fink, M. Gilbert, S. Chang, L. Junck, D. Schiff, F. Lieberman, H.A. Fine, M. Mehta, H.I. Robins, L.M. DeAngelis, M.D. Groves, V.K. Puduvalli, V. Levin, C. Conrad, E.A. Maher, K. Aldape, M. Hayes, L. Letvak, M.J. Egorin, R. Capdeville, R. Kaplan, A.J. Murgo, C. Stiles, and M.D. Prados. 2006. Phase I/II study of imatinib mesylate for recurrent malignant gliomas: North American Brain Tumor Consortium Study 99-08. *Clin Cancer Res*. 12:4899-907.

Yarden, Y., and M.X. Sliwkowski. 2001. Untangling the ErbB signalling network. *Nat Rev Mol Cell Biol*. 2:127-37.

Yung, W.K. 1989. In vitro chemosensitivity testing and its clinical application in human gliomas. *Neurosurg Rev*. 12:197-203.

Zhai, G.G., R. Malhotra, M. Delaney, D. Latham, U. Nestler, M. Zhang, N. Mukherjee, Q. Song, P. Robe, and A. Chakravarti. 2006. Radiation enhances the invasive potential of primary glioblastoma cells via activation of the Rho signaling pathway. *J Neurooncol*. 76:227-37.

Ziegler, D.S., A.L. Kung, and M.W. Kieran. 2008. Anti-apoptosis mechanisms in malignant gliomas. *J Clin Oncol*. 26:493-500.

9.   Acknowledgments – Danksagung

10.   Declaration of honour – Erklärung

Ich erkläre an Eides statt, dass ich die der Fakultät für Medizin der Technischen Universität München zur Promotionsprüfung vorgelegte Arbeit mit dem Titel:

"Targeting heterodimeric EGFR/ErbB2-receptor complexes with novel bispecific small-molecule tyrosine kinase inhibitors in combination with an experimental radiotherapy in human malignant glioma cells"

in der Fachabteilung Neuropathologie des Instituts für Allgemeine Pathologie und Pathologische Anatomie des Klinikums Rechts der Isar unter der Anleitung und Betreuung durch Univ.-Prof. Dr. med J. Schlegel ohne sonstige Hilfe erstellt und bei der Abfassung nur die gemäß § 6 Abs. 5 angegebenen Hilfsmittel benutzt habe.

Ich habe die Dissertation in keinem anderen Prüfungsverfahren als Prüfungsleistung vorgelegt. Ich habe den angestrebten Doktorgrad noch nicht erworben und bin nicht in einem früheren Promotionsverfahren für den angestrebten Doktorgrad endgültig gescheitert.

Die Promotionsordnung der Technischen Universität München ist mir bekannt.

Teile der vorliegenden Arbeit wurden als Kongressbeiträge präsentiert:

- Berezowska S., Grosu A.-L., Schlegel J. (2004):
Targeting heterodimeric EGFR/HER2 receptor complexes with a novel bispecific small molecule tyrosine kinase inhibitor enhances the effects of an experimental radiotherapy in human malignant glioma cells.
Internationales Symposium & Jahrestagung der Neuro-Onkologischen Arbeitsgemeinschaft (NOA) der Deutschen Krebsgesellschaft e. V., Düsseldorf 2004.
Abstract veröffentlicht in: J Neurooncol. 70:99.

- Berezowska S., Grosu A.-L., Diermeier-Daucher S., Schlegel J. (2008):
„Targeted" Therapie heterodimerer EGFR/HER2 Rezeptorkomplexe mit einem neuen bispezifischen „small molecule" Tyrosinkinase Inhibitor ist ein wirkungsvoller therapeutischer Ansatz in EGFR abhängigen humanen Glioblastomzellen.
92. Jahrestagung der Deutschen Gesellschaft für Pathologie e.V., Berlin 2008.
Abstract veröffentlicht in: Pathologe. 29(S1):58-59.

München, den ....
                                                                        Unterschrift

11.   Curriculum vitae

Name, Vorname:	Berezowska, Sabina Anna
Geburtsdatum/-ort:	03.12.1978, Krakau (Polen)
Staatsangehörigkeit:	deutsch
Familienstand:	ledig

Schulische Ausbildung:

1985 – 1989	Grundschule in München
1989 – 1998	Städtisches Michaeli-Gymnasium, München
Juni 1998	Abitur

Universitäre Ausbildung:

	Studium der Humanmedizin an der Technischen Universität München (WS 1998/99 – SS 2006)
WS 1998/99 – SS 2000	Vorklinischer Abschnitt – Klinikum Biederstein, München
18.08.2000	Ärztliche Vorprüfung
WS 2000/01 – SS2006	Klinischer Abschnitt – Klinikum Rechts der Isar, München
08/2001	1. Abschnitt der Ärztlichen Prüfung
03/2005	2. Abschnitt der Ärztlichen Prüfung

Praktisches Jahr:

06/2005 – 10/2005	PJ Innere Medizin – Universitätskrankenhaus New Royal Infirmary of Edinburgh (U.K.) und Universitätskrankenhaus der Universität Warschau (Polen)
12/2005 – 03/2006	PJ Chirurgie – Universitätskrankenhaus „Centro de Salud" der Universität Tucumán (Argentinien)
05/2006 – 08/2006	PJ Neurologie – Universitätsklinik, Inselspital Bern (Schweiz)
10/2006	3. Abschnitt der Ärztlichen Prüfung und Approbation

Beruflicher Werdegang:

Seit 04/2007	Assistenzärztin am Pathologischen Institut der Ludwig-Maximilians-Universität München

München, den ....
                                                          Unterschrift